UNIVERSIDADE TÉCNICA DO ATLÂNTICO
INSTITUTO DE ENGENHARIA E CIÊNCIAS DO MAR
WEST AFRICAN SCIENCE SERVICE CENTRE ON CLIMATE CHANGE AND ADAPTED LAND USE

Master Thesis

ASSESSING THE SPATIO-TEMPORAL VARIABILITY OF CHLOROPHYLL-A ACROSS CABO VERDE USING REMOTE SENSING DATA

KODJO OLIVIER ASSOKPA

Master Research Program on Climate Change and Marine Sciences

São Vicente
2023

UNIVERSIDADE TÉCNICA DO ATLÂNTICO
INSTITUTO DE ENGENHARIA E CIÊNCIAS DO MAR
WEST AFRICAN SCIENCE SERVICE CENTRE ON CLIMATE CHANGE AND ADAPTED LAND USE

Master Thesis

ASSESSING THE SPATIO-TEMPORAL VARIABILITY OF CHLOROPHYLL-A ACROSS CABO VERDE USING REMOTE SENSING DATA

KODJO OLIVIER ASSOKPA

Master Research Program on Climate Change and Marine Sciences

Supervisor | Dr. Elodie Martinez
Co-supervisor | Dr. Marie Bonnin

São Vicente
2023

UNIVERSIDADE TÉCNICA DO ATLÂNTICO

INSTITUTO DE ENGENHARIA E CIÊNCIAS DO MAR

WEST AFRICAN SCIENCE SERVICE CENTRE ON CLIMATE CHANGE AND ADAPTED LAND USE

Assessing the spatio-temporal variability of Chlorophyll-a across Cabo Verde using Remote Sensing Data

Kodjo Olivier ASSOKPA

Master's thesis presented to obtain the master's degree in Climate Change and Marine Sciences, by the Institute of Engineering and Marine Sciences, Atlantic Technical University in the framework of the West African Science Service Centre on Climate Change and Adapted Land Use

Supervisor

Dr. Elodie Martinez
Laboratory of Physical and
Space Oceanography (LOPS),
Brest, France

Co-supervisor

Dr. Marie Bonnin

UMR LEMAR, Brest, France

São Vicente
2023

UNIVERSIDADE TÉCNICA DO ATLÂNTICO

INSTITUTO DE ENGENHARIA E CIÊNCIAS DO MAR

WEST AFRICAN SCIENCE SERVICE CENTRE ON CLIMATE CHANGE AND ADAPTED LAND USE

Assessing the spatio-temporal variability of Chlorophyll-a across Cabo Verde using Remote Sensing Data

Kodjo Olivier ASSOKPA

Panel defense

President

Prof. Estanislau Lima

Examiner 1

Prof. Dr. Florian Schütte

Examiner 2

MSc. Elizandro Rodrigues

São Vicente
2023

Financial support

The German Federal Ministry of Education and Research (BMBF) in the framework of the West African Science Service Centre on Climate Change and Adapted Land Use (WASCAL) through WASCAL Graduate Studies Programme in Climate Change and Marine Sciences at the Institute for Engineering and Marine Sciences, Atlantic Technical University, Cabo Verde.

Dedication

I would like to dedicate this work to my family, who have been a great source of emotional support for me. In particular, I would like to express my deepest gratitude to my father, ASSOKPA Komi Agbémébia who has been always there for me and my five (5) siblings.

Acknowledgements

I would like to express my heartfelt gratitude to the Almighty God for blessing me with good health throughout the duration of this study.

I am deeply indebted to my supervisor, Dr. Elodie MARTINEZ from the Laboratory of Physical and Space Oceanography (Brest, FRANCE). Despite her busy schedule, she consistently had time, always providing guidance for me.

My sincere appreciation to my co-supervisor Dr. Marie Bonnin, from the Research Institute of Development (Brest, FRANCE) for her guidance throughout this master's project. Her presence and encouragement were invaluable. I would also like to express my gratitude for her warm welcome to Brest during my stay.

I extend my thanks to Dr. Corrine Almeida, the director of the WASCAL program at Instituto de Engenharia e Ciências do Mar (ISECMAR), for her continuous support, clarity, and guidance whenever needed. I would also like to express my appreciation to Dr. Estanislau Baptista Lima, the scientific coordinator, for his encouragement. I am also grateful to Dr. Antonio Pinto, the Deputy Director, and the entire WASCAL staff.

My gratitude goes to my colleague and dear friend Wise Goodluck DATSOMOR from Ghana for his friendship and emotional support during this journey.

Lastly, I am grateful to my fellow colleagues of the WASCAL Cabo Verde third batch. Their friendship during this journey has been truly exceptional and has made us one family.

Resumo

A clorofila-a (Chl-a) é utilizada como um indicador para estimar a biomassa do fitoplâncton que, enquanto base da cadeia alimentar marinha, desempenha um papel crucial na avaliação da saúde e da produtividade dos ecossistemas marinhos. Este estudo tem por objetivo avaliar a variabilidade sazonal e interanual da Chl-a e investigar alguns mecanismos subjacentes a estas alterações. Utilizando imagens de satélite MODIS-Aqua, captadas mensalmente com uma resolução de 4 km, o estudo fornece informações sobre a distribuição espácio-temporal da Chl-a e da temperatura da superfície do mar (SST). Os resultados revelam padrões sazonais distintos, com o máximo de Chl-a a ocorrer em janeiro (cerca de 0,32 mg/m^3) e valores mínimos observados em agosto (aproximadamente 0,15 mg/m^3) em Cabo Verde. Estas variabilidades sazonais na Chl-a são acompanhadas por alterações correspondentes na SST, com temperaturas máximas a ocorrer em setembro (cerca de 27 °C) e temperaturas baixas em janeiro (aproximadamente 23 °C). A análise também identifica anos anormais, como 2010, 2011, 2015 e 2018, caracterizados por desvios dos padrões médios sazonais de Chl-a. Além disso, observa-se uma mudança de regime na Chl-a a partir de 2013, com uma tendência geral de aumento até 2022. Além disso, a análise demonstra a relação entre a variabilidade da Chl-a e da SST nos pequenos pelágicos e no atum, respetivamente. Estes resultados podem ajudar as partes interessadas na pesca sustentável e na conservação em Cabo Verde. Uma maior integração das variáveis ambientais pode melhorar os modelos de previsão e a compreensão da dinâmica da Chl-a em Cabo Verde.

Palavras-chave: Fitoplâncton, concentração de clorofila-a, temperatura da superfície do mar, variabilidade espácio-temporal, Arquipélago de Cabo Verde.

Abstract

Chlorophyll-a (Chl-a) is used as a proxy to estimate the biomass of phytoplankton which, as the base of the marine food web, plays a crucial role in assessing the health and productivity of marine ecosystems. This study aims to evaluate the seasonal and interannual variability of Chl-a and investigate the parallel changes in SST as an indicator of some physical process in the ocean. By using satellite imagery from MODIS-Aqua, captured monthly at a 4 km resolution, the study provides insights into the spatio-temporal distribution of Chl-a and Sea Surface Temperature (SST). The results reveal distinct seasonal patterns, with maximum Chl-a occurring in January (around 0.32 mg/m³) and minimum values observed in August (approximately 0.15 mg/m³) in Cabo Verde as well as an inverse relationship between Chl-a and SST. These seasonal variabilities in Chl-a are accompanied by corresponding changes in SST, with peak temperatures occurring in September (around 27 °C) and low temperatures in January (approximately 23 °C). The analysis also identifies abnormal years, such as 2010, 2011, 2015, and 2018, characterised by deviations from the seasonal average Chl-a patterns. Additionally, a regime shift in Chl-a starting in 2013 is observed, with an overall increasing trend until 2022. Furthermore, the analysis demonstrates the relationship between Chl-a and SST variability in small pelagic fish and tuna respectively. These findings can help stakeholders for sustainable fishing and conservation in Cabo Verde. Further integration of environmental variables can enhance models predictive and the understanding of Chl-a dynamics in Cabo Verde.

Keywords: Phytoplankton, Chlorophyll-a concentration, Sea Surface Temperature, Spatio-Temporal variability, Cabo Verde Archipelago.

Abbreviations and acronyms

ANETUS	Atlantic North-eastern Tropical Upwelling System
CC	Canary Current
CCUS	Canary Current Upwelling System
CDOM	Coloured Dissolved Organic Matter
Chl-a	Chlorophyll-a
CMEMS	Copernicus Marine Environment Monitoring Service
CO_2	Carbon Dioxide
CV	Cabo Verde
EAO	Equatorial Atlantic Oscillation
EEZ	Exclusive Economic Zone
ENSO	El Niño-Southern Oscillation
HNLC	High Nutrient Low Chlorophyll
IME	Island Mass Effect
IMar	Instituto do Mar
ITCZ	Intertropical Convergence Zone
JFA	Juan Fernández Archipelago
MEI	Multivariate ENSO Index
MODIS	Moderate-Resolution Imaging Spectroradiometer
O_2	Dioxygen
NACW	North Atlantic Central Water
NEC	North Equatorial Current
NECC	North Equatorial Counter Current
NKP	North Kerguelen Plateau
NO_3	Nitrate

NPP	Net Primary Productivity
OC-CCI	Ocean Color Climate Change Initiative
PAR	Photosynthetically Available Radiation
PF	Polar Front
PO_4	Phosphate
SACW	South Atlantic Central Water
SeaWiFS	Sea-viewing Wide Field-of-view Sensor
SST	Sea Surface Temperature
SSW	South-Southwest
TIWs	Tropical Instability Waves

List of contents

Figure index

Table index

1. Introduction

The oceans cover more than 70% of the earth's surface. These vast expanses of water are not only home to abundant marine life but also have a considerable influence on the Earth's climate. The relationship between ocean ecosystems and global climate change is attracting much attention (Spring, 2019; Siswanto et *al.*, 2020). As the base of the marine food web, phytoplankton plays a fundamental role in the biogeochemical cycling of elements by converting inorganic elements into organic components. Phytoplankton are advected microalgae and therefore dependent on marine currents. They can photosynthesize using light and nutrients such as NO_3 (Nitrate), PO_4 (Phosphate), Si (Silicate), Fe (Iron) and carbon dioxide (CO_2) available in the water to produce oxygen and organic matter. As primary producers of the sea, a lot of marine organisms, including fish, depend on them for their nutrition. They also contribute also to roughly half of the fixed carbon on the planet by absorbing atmospheric CO_2 and producing 50% of dioxygen (O_2) essential for life on the earth's surface (Martin, 2014). In the current scenario of climate change, a noticeable decrease in primary production on a larger scale has been observed. (Boyce et *al.*, 2010).

Chlorophyll-a is the pigment found in algae and other photosynthetic organisms. The concentration of Chl-a is an indicator of the biomass of phytoplankton in the ocean ecosystem (Behrenfeld & Falkowski, 1997). Estimating the number of microscopic phytoplankton and associated primary productivity over large ocean areas is extremely difficult for ships (Dierssen & Randolph, 2012). However, satellite remote sensing of ocean color has provided a reliable data source to study phytoplankton dynamics from intra to interannual timescales (Vantrepotte & Mélin, 2009; Krasnopolsky et *al.*, 2016). And so, Chl-a is one of the seawater components that are detected from space using ocean color techniques. SST can have an indirect impact on Chl-a by physiologically influencing marine organisms and acting as an indicator of the physical processes that modulate nutrient availability. And so, high SST reinforces ocean stratification which limits vertical mixing and upwelling of nutrients needed by phytoplankton. In addition, high SST accelerates the metabolisms of marine organisms, impacting their physiology and population dynamics, including that of phytoplankton and consequently Chl-a which is used as a proxy. These processes will be reversed with low SST. El Niño-Southern Oscillation (ENSO) can also affect Chl-a, with El Niño events reducing and La Niña events increasing concentrations which can be all the way round depending on the region (whether in the open ocean or in the coastal area). Satellite remote sensing helps monitor these parameters, while climate change alters SST and nutrient availability, affecting Chl-a and ecosystem

dynamics. Changes in Chl-a and SST have cascading effects on marine ecosystems, affecting higher trophic levels and biodiversity.

Wind speed also affects Chl-a in the ocean. When the strong wind can mix the water and bring nutrients up from the depths to the surface (Masunaga & Schneider, 2022). This phenomenon, known as wind-induced upwelling, favours the availability of nutrients and consequently the growth of phytoplankton. On the other hand, powerful winds can hinder phytoplankton growth. Although it may seem beneficial at first sight, this upwelling can actually limit the development of phytoplankton. Deep waters are often too cold for optimal growth, with phytoplankton thriving in warmer conditions. In addition, turbulent mixtures can drag phytoplankton to great depths, depriving them of the light necessary for photosynthesis. The impact of winds depends on their duration, intensity and the specific phytoplankton species present (such as diatoms and dinoflagellates, whose single-cell structure makes them more sensitive to cold water and change).

Rainfall can temporarily affect Chl-a by diluting Chl-a in water, decreasing its concentration. This dilution effect occurs when rainwater mixes with the surface water, reducing the overall Chl-a. This can be particularly evident in areas with low initial nutrient levels, where the dilution effect of rainfall can have a more pronounced impact (Shafeeque et *al.,* 2019). Heavy rainfall events can bring nutrients into the water though land draining, stimulating the phytoplankton growth. When rainfall delivers these nutrients to the water, it can enhance the availability of resources for phytoplankton, leading to an increase in Chl-a levels.

Chl-a is one of the reliable indicators of global fishery yields (Friedland et *al.,* 2012). It reflects the export of energy from the pelagic food web to higher trophic levels. Changes in Chl-a levels can have a direct impact on the abundance and distribution of phytoplankton, subsequently influencing the availability of food resources for fish. Higher Chl-a indicates increased phytoplankton productivity, providing more prey for zooplankton and small fish. This food abundance can lead to larger fish populations and higher fishing yields. On the contrary, low Chl-a can indicate a decline in phytoplankton productivity, leading to a reduction in available food and potentially lower fish populations and fisheries productivity.

The Cabo Verde (CV) archipelago, the focus area of this study, presents diverse hydrographic conditions due to the confluence of some ocean currents and the proximity of coastal upwelling. However, the islands are mainly located in the inter-gyre region between

the west oligotrophic zone and east mesotrophic zone near the African coast. The Canary Current (CC) and the North Equatorial Current (NEC) are the main surface currents influencing the archipelago. On the other hand, the southern side of the islands is seasonally influenced by the NECC due to the movement of the Intertropical Convergence Zone (ITCZ), which produces changes in the wind regime (Ramos et *al.*, 2012). And so, a crucial frontal zone occurs near the archipelago mixing NACW and SACW (North Atlantic Central Water and South Atlantic Central Water).

The literature has shown a large-scale decrease in Chl-a around CV from 1992 to 2005 (Lathuilière et *al.*, 2008), especially during 2000-2004 (Ramos et *al.*, 2012). The actual spatio-temporal variability of Chl-a and the trend are still unknown causing the problem of a lack of knowledge about the dynamics of Chl-a. There is also a lack of study about how the Island Mass Effect (IME) can affect the phytoplankton enrichment around CV. The IME encompasses a range of biological and physical processes near islands and reefs, characterized by plumes of concentrated Chl-a detected upstream and propagating downstream. And so, two questions will be addressed in this work to solve this problem. Firstly, what are the seasonal and interannual variability of Chl-a across CV Island? And secondly, what is the parallel relationship with SST variability?

Objectives of the work

The main purpose of this study is to evaluate the phytoplankton enrichment variability over CV Archipelago. Specifically, it aims:

- To characterize the seasonal and interannual variability of Chl-a and the trend based on analysis of satellite images over 20 years from 2002 to 2022.
- To investigate the parallel changes in SST as an indicator of some physical process in the ocean.

The study of Chl-a variability in CV is essential for understanding the health and productivity of the marine ecosystem, supporting sustainable fishing. It also allows assessing the impacts of climate change, managing coastal tourism and recreational activities, and ensuring the security of water resources. The results can be used by stakeholders, including policymakers, environmental agencies, fisheries managers, tourism operators and local communities, to make informed decisions and implement effective management strategies.

2. Literature review

Studies have highlighted environmental factors such as SST, wind speed on phytoplankton growth and nutrient availability, ultimately impacting fisheries' productivity and distribution in marine ecosystems.

2.1. Variability of Chl-a around Islands

Chavez et *al.* (2011) has shown the increase in global marine primary production in recent decades. They also discussed how recent in situ and satellite time series of primary production can be linked to interannual variability in the ocean. The increase in phytoplankton around small islands has been documented worldwide (Falco et *al.*, 2022). This increase has been reported since the late 1950s and is known as the IME (Doty and Oguri, 1956). According to Hamne and Hauri (1981), IME refers to a spectrum of biological and physical processes in the immediate vicinity and downstream of islands and reefs (Cardoso et *al.*, 2020). Martinez and Maamaatuaiahutapu (2004) studied phytoplankton blooms in the Marquesas Islands during the period of Sea-viewing Wide Field of View Sensor (SeaWiFS) activity, from September 1997 to February 2002. They showed that bloom was explained by the dynamic interaction of circulation and topography.

Gove et *al.* (2016) focused on coral reefs, proving that IME is an almost ubiquitous feature in 91 % of tropical Pacific coral reef ecosystems, creating 'hotspots' of phytoplankton biomass throughout the upper water column near islands, also known as oceanic oases. According to Doty & Oguri (1956), phytoplankton productivity increases steadily as one approaches the coasts of oceanic islands, which is attributed to the IME. Jena (2016) investigated the phenomenon of IME using remote sensing observations on the sub-Antarctic shelf of Kerguelen in the Southern Ocean. He analyzed climatological Chl-a datasets from the Moderate Resolution Imaging Spectroradiometer (Aqua-MODIS) and the SeaWiFS to characterize the increase in surface area in the downstream section of the shelf along the Polar Front (PF). The results showed distinct plumes (Chl-a > 0.5 mg/m^3) during the austral spring-summer propagating up to~1800 km offshore to 98 °E along the downstream northern section of the NKP (North Kerguelen Plateau). Satellite remote sensing data sets are well suited to observing and quantifying the seasonal extent of phytoplankton blooms.

Messié et *al.* (2022) discuss a new type of IME called "delayed IME" which occurs when diazotrophs slowly use excess phosphate and iron after a classical island effect while being advected away from islands. The fertilizing impact of islands on phytoplankton may

therefore be largely underestimated in the oligotrophic ocean. Andrade et *al.* (2014) showed that IME is a recurrent feature affecting both local and regional scales in the Juan Fernández Archipelago (JFA). However, they did not explore the potential impacts of climate change or human activities on IME.

Chl-a variability was characterized by Lathuilière et *al.* (2008) on seasonal and intra-seasonal time scales along the northwest coast of Africa from 1992 to 2005 using SeaWiFS ocean color data. They found a large-scale decrease in Chl-a concentration Chl-a around CV.

2.2. Some mechanisms that affect Chl-a

Ramos et *al.* (2012) found that the seasonal and interannual variability of phytoplankton concentration in the Cabo Verde region is influenced by a synergy of factors that vary according to the general oscillation of physical parameters in the subtropical North Atlantic. The distribution of Chl-a showed a strong increase during October and November, followed by a less pronounced increase during February in certain locations around the islands. This is linked to the arrival of water from upwelling systems, the seasonality of the monsoon, geostrophic circulation and mesoscale structures in the region. Interannual analysis shows a decreasing trend in Chl-a in the area. It is also linked with the presence of Sahara Dust in winter. Dust particles from the Sahara Desert in North Africa affect Cabo Verde at surface level from October to March (Gama et *al.*, 2015). Dust can have a positive impact on marine ecosystems, as it contains nutrients such as iron, which can stimulate the growth of phytoplankton.

2.2.1. Relationships between Sea Surface Temperature (SST) and Chl-a

In their research, Pradhan et *al.* (2006) explored the variability of Chl-a in the Mauritanian upwelling, establishing a strong link between Chl-a and SST. They observed that Chl-a is high during winter and spring when SST is lower, and conversely, Chl-a decreases as SST increases during summer and autumn. This inverse relationship has been explained by the effect of convection which tends to be more active in winter and spring. In addition, this study highlighted interannual fluctuations, in particular the anomalous 1998-1999 event, attributed to the El Niño-Southern Oscillation (ENSO), which resulted in low Chl-a levels alongside high SST values. Falco et *al.* (2022) found that the IME results in different SST regimes depending on the size and altitude of the islands, with large islands showing upwelling/downwelling zones and small islands showing local cooling due to interactions between currents and islands. IME also leads to the formation of shadow zones, which causes the stratification and warming of

surface waters and a reduction in net primary productivity (NPP). Martinez and Maamaatuaiahutapu (2004) also observed a strong correlation between SST and Chl-a.

Martinez et *al.* (2018) studied 18 years (1997 – 2014) of satellite images, ocean data reanalyses and Lagrangian diagnostics to characterize the high biological activity in the Marquesas. They discussed the influence of tropical instability waves (TIWs) on phytoplankton biomass near the Marquesas Islands in the Pacific Ocean. Thus, they showed that SST and phytoplankton are negatively correlated in the Marquesas archipelago, meaning that lower SST is linked to higher phytoplankton concentration. However, they suggested that the increase of phytoplankton during La Niña events may not be caused by TIWs bringing iron-rich waters from the equator, but rather by local processes such as thermocline uplift or coastal upwelling induced by stronger trade winds. Therefore, SST is not a direct driver of phytoplankton variability, but rather an indicator of TIW activity and large-scale forcing in the region. Finally, they concluded that whatever the conditions, the influence of tropical instability waves (TIWs) is to disperse, stir up and, therefore, modulate the shape of the existing phytoplankton plume.

Behrenfeld et *al.* (2006) found a strong correspondence between multivariate ENSO index (MEI) variability and NPP anomalies, indicating that climate effects on ocean biology are mediated by changes in upper ocean temperature and stratification, which influence the availability of nutrients for phytoplankton growth. They have shown that surface warming in permanently stratified ocean regions is accompanied by reductions in productivity. Caldeira et *al.,* (2002) found that changes in global ocean NPP over the last decade are due to changes in the permanently stratified low-latitude oceans and are closely linked to coincident climate variability.

Faye et *al.,* (2015) investigated the climatological seasonal cycle of sea surface temperature (SST) in the northeastern tropical Atlantic (7-25 ◦N, 26-12 ◦W) using a mixed layer heat balance in a regional ocean general circulation model. The region, which experiences one of the extensive SST cycles in the tropics, forms the central part of the Guinea Gyre. They concluded that the relationship between SST and phytoplankton growth is not linear or uniform, as other factors, such as light availability, nutrient supply, grazing pressure, and horizontal advection, also influence the phytoplankton dynamics. Therefore, SST is not a direct proxy for Chl-a, but rather a useful variable to understand the physical processes that affect the marine ecosystem in the Atlantic North-Eastern Tropical Upwelling System (ANETUS).

Fernández-González et *al.* (2022) conducted four microcosm experiments in the tropical and subtropical Atlantic, where phytoplankton communities were exposed to different combinations of SST and nutrient conditions. They found that nutrient supply has a much larger effect than SST on phytoplankton growth and biomass, and that the effect of SST is reduced under nutrient-limited conditions. They also found that phytoplankton assemblages from warmer regions are not more vulnerable to increased SST, and that warming may enhance their ability to exploit nutrient injections. They suggested that the low temperature sensitivity of phytoplankton growth in oligotrophic regions may be due to ecological and physiological constraints, such as grazing pressure, low cell abundance, and depleted nutrient quotas.

2.2.2. Impacts of Wind Speed on Chl-a

Cassianides et *al.* (2020) carried out research to explain the physical mechanisms involved in the phytoplankton blooms observed in the north and south of the Marquesas archipelago, a region where the waters are rich in nutrients and poor in Chl-a (HNLC). A combination of satellite observations and 2D Lagrangian simulations was used to illustrate the role of island fertilization and mesoscale oceanic activity in these events. The Lagrangian simulations highlighted the key role of surface currents in the spatial coverage and dispersion of Chl-a plumes from the islands. The Chl-a plumes revealed contrasting dynamic regimes in the archipelago, with more mesoscale eddies in the south and smaller-scale dynamic activity in the north.

Lázaro et *al.* (2005) detected and described the seasonal patterns of the main current systems in the CV region, such as the North Equatorial Counter Current, the Mauritania Current, the Canary Current, the North Equatorial Current, and the Guinea Dome, using satellite altimetry data. They concluded that the phytoplankton blooms were triggered by the upwelling of nutrient-rich water induced by the negative Sea Surface Height (SSH) anomalies associated with the Equatorial Atlantic Oscillation (EAO) cold phase. The upwelling was enhanced by the seasonal relaxation of the trade winds and the northward shift of the ITCZ.

Fernandes et *al.* (2005) provided a characterization of the main current systems in the northeast tropical Atlantic and their variability, seasonal distribution of SST and Chl-a by analyzing a time series of remote sensing data. Demarcq & Somoue, (2015) examined the factors determining phytoplankton net primary production (NPP) in the Canary Current Upwelling System (CCUS), one of the most productive coastal upwelling systems in the world.

2.3. Relationships between Chl-a, SST, and Fisheries

Friedland et *al.* (2012) identified different environmental factors that affect the fishery yields of 52 large marine ecosystems (LMEs) around the world. They found that net primary production (NPP), a measure of the amount of organic matter produced by phytoplankton, is not a good predictor of fishery yields at a global scale. And so, suggests that other factors, such as Chl-a, particle export ratio, and mesozooplankton productivity, are more important for determining the transfer of energy from primary producers to higher trophic levels and ultimately to fishery yields. Furthermore, they showed that fishery yields are influenced by temperature and latitude, with higher yields associated with colder and higher latitude ecosystems.

Erauskin-Extramiana et *al.* (2019) presented the results of their models, showing historical trends and future projections of tuna distribution and relative abundance. They indicated that most tuna species have shifted poleward in response to environmental changes, and that larger shifts are expected by the end of the century. They also showed that temperate tuna and bigeye tuna are expected to decline in the tropics and move towards the poles (Andrade & Garcia, 1999), while skipjack and yellowfin tuna are expected to become more abundant in tropical areas and in the EEZ (Exclusive Economic Zone) of most coastal countries.

Li et *al.* (2014) provided valuable information on the distribution patterns and environmental influences on chub mackerel in China's coastal waters. By combining fisheries and remote sensing data, the study helps to better understand where chub mackerel are likely to be found and how environmental factors play a role in their habitat preferences.

Understanding Chl-a variability in CV using remote sensing is very important because there is not enough research on this subject. Chl-a is a key factor in determining the health and productivity of marine ecosystems. CV has amazing coastal ecosystems and valuable marine resources that need to be looked after. That is why it is important to keep a close eye on Chl-a in these waters to make sure that all is well. Thanks to remote sensing, we can cover vast areas and track changes over time without breaking the bank. This study is noteworthy because it can fill in the gaps and help us better understand how Chl-a levels change throughout the year and in different places in the waters of CV may be related with changes in fisheries. This means smarter decisions to protect these magnificent marine environments and keep them thriving for the future.

3. Materials and Methods

3.1 Study site

The CV archipelago is located on the eastern edge of the North Atlantic, about 450-600 km of the west coast of Africa and 1400 km South-southwest (SSW) of the Canary Islands. It is limited by parallels 14◦40' and 17◦30' of north latitude and through meridians 21◦30' and 25◦300' of west longitude. The archipelago is formed by ten islands, nine of which are inhabited, and thirteen islets, which occupy a total area of 4033 km^2 and an exclusive economic zone (EEZ) that extends over approximately 700,000 km^2 (Morais et al., 2021). The current population of CV is 571,191 as of Tuesday, January 10, 2023, based on Worldometer elaboration of the latest United Nations data. The archipelago has a maximum elevation of 2829 m on Fogo Island; geologically, it is made up of sub-aerial, predominantly basaltic, emissions from lava flows and pyroclastic materials (i.e., slag, bagacin, or lapilli and ash). Therefore, soils are generally coarse-textured and thin, with a reduced ability to retain water. Globally, CV has an average temperature of 25 ◦C, presenting, like other Sahelian countries, two seasons: A dry season, from December to June, and a wet season, from August to October. July and November are considered transitional months. More than 75 % of the average annual precipitation, around 300 mm, occurs in August and September. However, the CV archipelago presents islands with a predominantly arid climate and others with a predominantly semi-arid climate. The rainy season has an average duration of 15 to 25 days in the arid areas, and 45 to 55 days in the semi-arid areas (Morais et *al.*, 2021). Being situated in close proximity to the West coast of Africa, the CV Islands experience the effects of coastal upwelling, distinct from the local upwelling around the islands, as depicted in Figure 1.

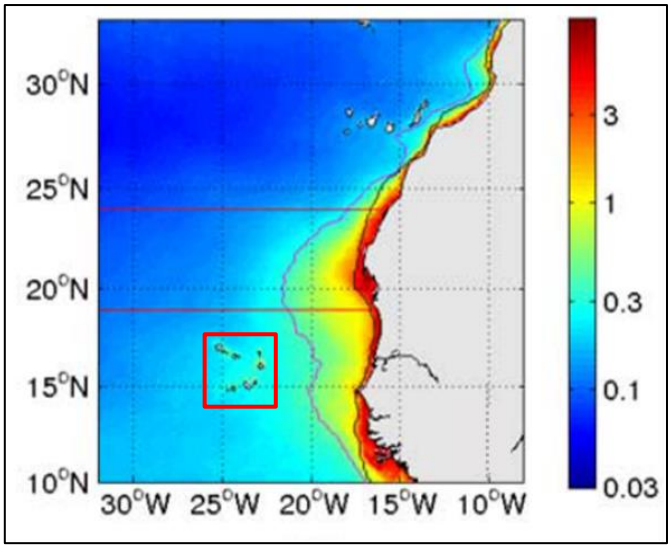

Figure 1 : Surface Chl-a (mg/m^3), derived from SeaWiFS with 9 km resolution, the red square superimposed CV islands, the African coast productive in red color which gradually degrades towards the open sea in blue colour as well as a signal of productivity around the islands of CV (Lathuilière et *al.*, 2008).

3.2. Surface current around Cabo Verde

The large-scale circulation around CV is dominated by the eastern branch of the North Atlantic subtropical gyre, which consists of the Azores Current, the Portugal Current, the CC and the North Equatorial Current (NEC) as shown in Figure 2. North of 22 °N, the large-scale circulation along the coast is directed southward in the subtropical gyre. South of 20 °N, a cyclonic recirculation gyre drives a predominately poleward circulation along the coast, as unlike the coastal jet. The equatorial current system influences the recirculation gyre. Its southern branch is fed by the eastward-flowing North Equatorial Counter Current (NECC). The position of this current has a large seasonal cycle. It is located near 5 °N in winter and reaches 10 °N in the summer. Thus, the coastal boundary deflects the NECC during summer, and a large part of the flow is directed poleward along the shore. In winter, the NECC flows eastward, south of the African peninsula into the Guinean Gulf. The CV Frontal zone separates the subtropical gyre and the recirculation gyre.

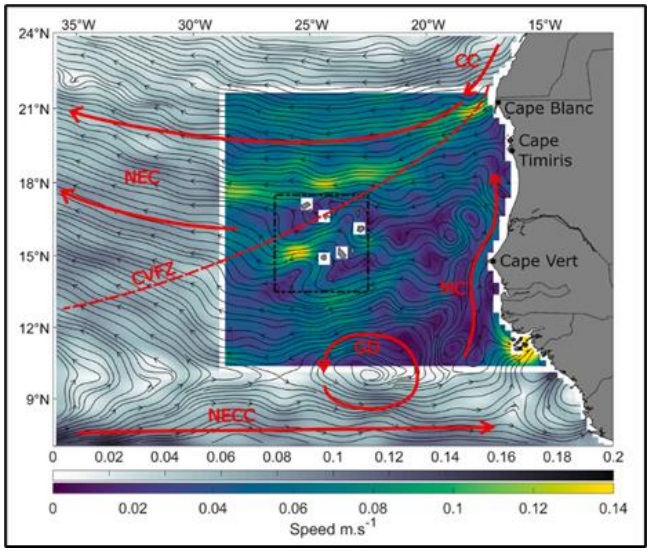

Figure 2: Mean surface ocean currents and features, the red lines represent the direction of the surface currents and the red dotted line represents the front of the CV, the black dotted line represents the islands of the CV (Cardoso et *al.*, 2020).

3.3. Bathymetry and topography

CV is a horseshoe-shaped archipelago facing west, made up of two main groups: the Windward Islands (north) and the Leeward Islands (south) (Ramalho, 2011). The islands can be divided into a northern chain (Santo Antão, São Vicente, Santa Luzia and São Nicolau) and a southern chain (Sal, Boa Vista, Maio, Santiago, Fogo, and Brava). Bathymetry reveals shallow areas and seamounts around the islands. The eastern islands have a flat topography, while the western islands are higher. The size of the archipelago varies from island to island, with Santiago being the largest and Santa Luzia the smallest. Distances between islands range from 8 to 270 kilometres.

3.4. Data

The study used monthly Chl-a[1] and SST[2] products from Aqua-MODIS Level 3, with a spatial resolution of 4 km from 2002 to 2022. Of all the ocean color sensors available, MODIS is currently the most widely used for studying ocean biology (Muskananfola et *al.*, 2021). The data were tested and validated using in situ measurements for several studies.

Satellite images of Chl-a and SST were used to produce monthly and annual mean surface maps and Hovmöller diagrams. A Hovmöller diagram is a handy graph used in earth

[1] https://hermes.acri.fr/index.php?class=archive
[2] https://oceancolor.gsfc.nasa.gov

sciences to track how a particular variable changes over time and along specific lines of longitude or latitude, allowing to spot patterns and trends in the data across different locations and periods. These images were also used to generate time series for analyses of temporal variability. Annual data from the the Institute of Marine Research (IMar), was used to assess the impact of variability in Chl-a and SST on the catch of tuna and small pelagic fish in particular. The data concern the comparative evolution of artisanal and industrial fisheries landings by species group from 1999 to 2022 (in tons).

3.5. Methods

The satellite images were analyzed using Python programming language to evaluate Chl-a and SST's spatiotemporal variability and conduct time series analysis. Since the year 2002 is not complete it was removed before the time series analysis. The localization map was made by QGIS software. The average maps were computer based on the schematic (Figure 3). They were calculated (for the whole 2003 - 2022 period, as well as for each month in the same multi-annual period) using the following equation:

$$\underline{X}(x,y) = \sum_{i=1}^{n} Xi(x,y,ti) \qquad (Eq: 1)$$

Where:

- $\underline{X}(x, y)$ is the monthly mean value or monthly climatology value at position (x, y);
- $Xi\ (x, y, t)$ is the t^{ith} value of the data at (x, y) position,
- n is the number of monthly data used to calculate the monthly climatology (i.e., from 2002 to 2022 = 20 months of January, 20 months of February …) and annual climatology (from 2002 to 2022 = 20 x 12). If *Xi* is an empty pixel, that pixel is not considered.

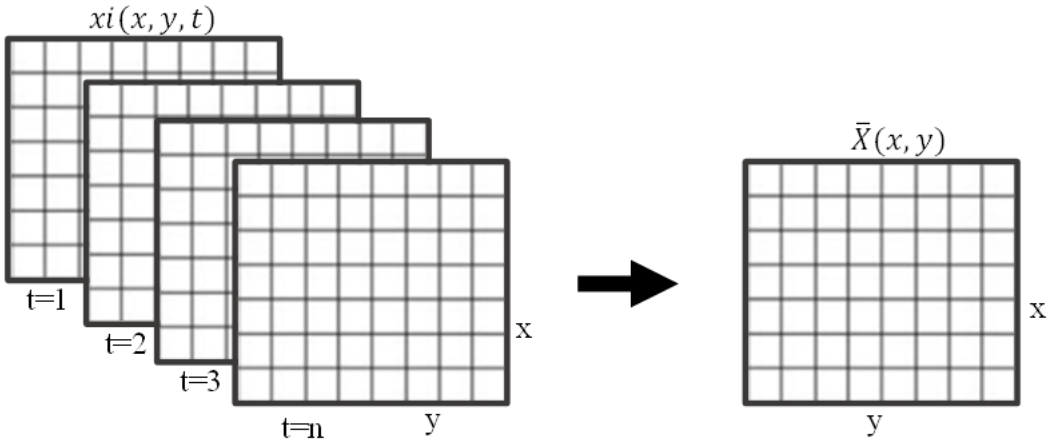

Figure 3: Schematic of the approach used to compute the (2002 - 2022) annual/monthly mean map for the Chl-a and the SST images, the small squares inside the satellite images represent pixels containing values dependent on the Chl-a or SST signal (source: Kodjo Olivier ASSOKPA, 2023).

In this study, three distinct boxes, each painted in different colors (red, blue, and black) were defined, all crafted to be the same size. These boxes were positioned to evaluate the distribution of productivity in three key zones: the oligotrophic zone, the CV Island, and the high productivity zone downward the Senegalese coastal upwelling region. The three zones are outlined in a 3 ° × 2.8 ° box, aligned with the unique shape of the CV archipelago. This approach ensures consistency for representation and comparison between the different zones. In addition, six stations were defined within the CV area. Four stations were positioned closely to the island locations further north, while an additional two stations were located far from the Islands not far from the equator. This arrangement aims to evaluate the islands' influence on productivity and the relation between SST and Chl-a in CV water.

The correlation analyses were carried out using the Pearson correlation which assesses the linear relationship between two continuous variables. It measures the strength and direction of the linear relationship using a scale from -1 to 1. A correlation of +1 indicates a perfect positive correlation, -1 indicates a perfect negative correlation, and 0 indicates no linear correlation. The equation is the following one:

$$r = \frac{n\sum XY - \sum X \sum Y}{\sqrt{\left(n\sum X^2 - \left(\sum X\right)^2\right) * \left(n\sum Y^2 - \left(\sum Y\right)^2\right)}} \qquad (Eq: 2)$$

Where:

- n is the number of observations,
- $\sum XY$ is the sum of the product of the x-value and y-value for each monthly data,

- $\sum$ X is the sum of the x-value,
- $\sum$ Y is the sum of y-values,
- $\sum$ X^2 is the sum of the squares of the x-values and
- $\sum$ Y^2 is the sum of the squares of the y-values.

Main Python Packages Used

We ran experiments on a computer with hardware specifications, shown in Table 1. Additionally, the language of Python programming, and several Python packages such as Numpy, Pandas, Cartopy, Matplotlib, and Sklearn were used for data analysis.

Table 1: Hardware and Python packages specifications

Components	**Specification**
Memory	16384 MB RAM
Processor	11th Gen Intel(R) Core (TM) i7-1185G7 @ 3.00GHz 1.80 GHz
Disk Capacity	500 GB
Operator System	Windows
Operator System Type	64-bit
Python Packages	Numpy, Pandas, Matplotlib, Sklearn, Seaborn, SciPy, Cartopy.

4. Results

4.1. Regional Variability of Chl-a and SST

4.1.1. Variability of Chl-a

The monthly average of satellite images of Chl-a from Modis-Aqua for 2002-2022 was used to assess the variability of Chl-a around Cabo (Figure 4). It provides valuable information on the spatial and temporal distribution of Chl-a c in the study area, which extends from the African coast to the open ocean (-30° West). Figures 4a and 4b show the analysis of the mean surface Chl-a map and the time series of interannual Chl-a data, respectively. The monthly percentage of missing values for satellite images of Chl-a for the three boxes, as shown in Figure 5, reveals a notable concentration of missing data, mainly during the summer months. To better understand the different Chl-a enrichment scenarios, three boxes of identical size were defined: a black box, a red box and a blue box (Figure 4a) in 3 contrasted regions.

The result reveals distinct patterns of Chl-a, highlighting the spatio-temporal variability of Chl-a at the surface. Of the three boxes, the black box representative of the upwelling region stands out as having consistently higher Chl-a, ranging from 1 to 5 mg/m^3, than the red and blue boxes. This high concentration in the black box indicates a region of increased phytoplankton biomass and productivity.

In contrast, the blue box in the extreme north-west shows no Chl-a signal with 0 mg/m^3. This indicates a region of low phytoplankton biomass and low productivity (oligotrophic).

The red box around the CV archipelago, located between the black box (productive zone) and the blue box (non-productive zone) and lower latitude, shows intermediate concentrations of Chl-a ranging from 0.1 to 1 mg/m^3. This indicates a moderate level of biomass and phytoplankton productivity in this region. The presence of CV Island plays a vital role in the productivity observed.

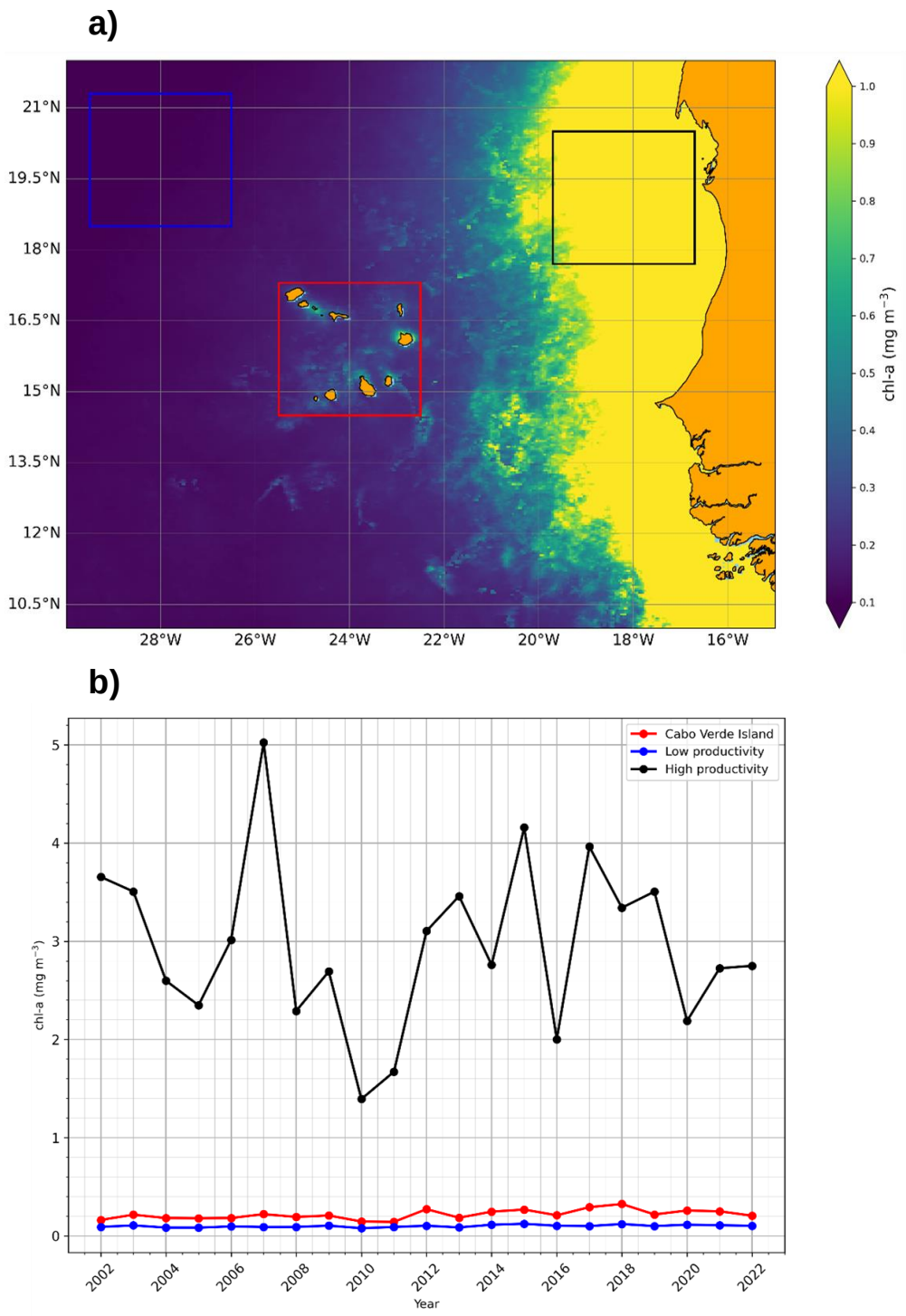

Figure 4: Chl-a concentration variability around CV from Modis-Aqua satellite images. (a) Mean surface Chl-a map from 2002 to 2022 over African coast including the CV Islands from Modis-Aqua product (in mg/m^3). The three boxes (Black, red, blue) represent contrasted regions of Chl-a. (b) Variability of mean Chl-a values for the three boxes from 2002 to 2022 (the open ocean in blue curve, the CV in red curve and the high productive near the African coast in black curve).

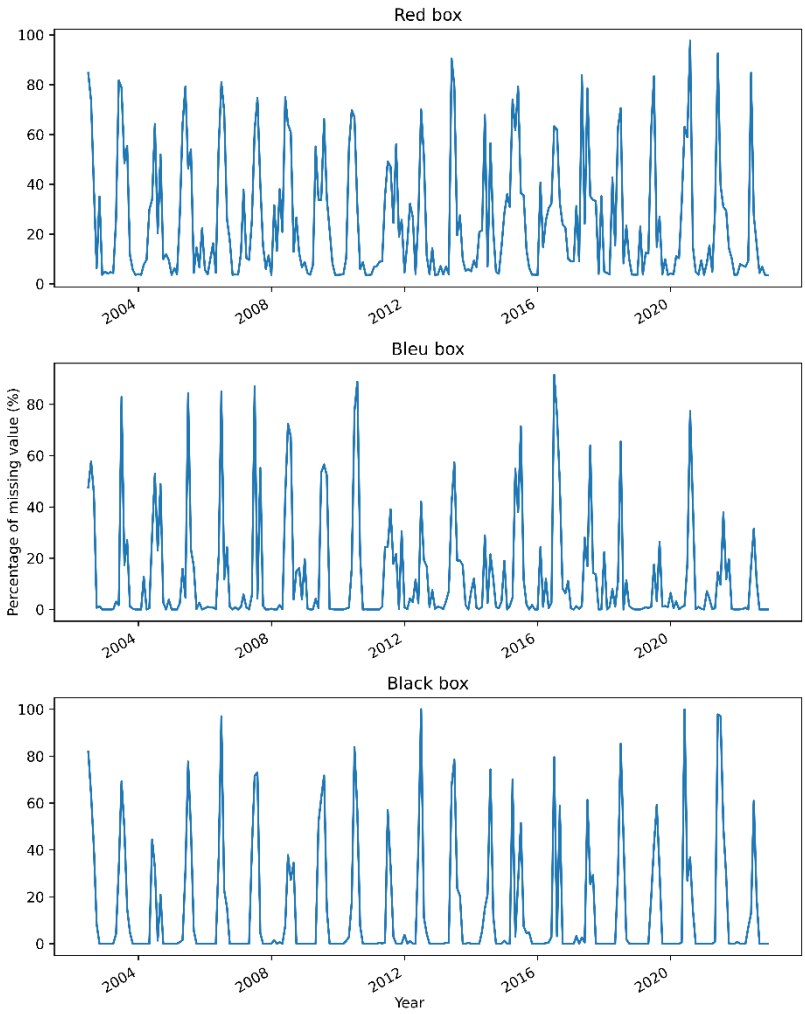

Figure 5: Percentage of missing value in the monthly Chl-a satellite image from 2002 to 2022 for the three boxes.

4.1.2 Variability of SST

The variability of SST around CV was assessed using the monthly mean of Modis-Aqua satellite images for 2002-2022 (Figure 6). Analysis of these images provides valuable information on the spatial and temporal distribution of Chl-a concentrations in the study area. More specifically, Figures 6a and 6b show the map of mean surface SST and the time series of interannual SST data, respectively. Figure 7 shows the monthly percentage of missing values for SST satellite images lower than 2 %. Firstly, there is a latitudinal and longitudinal variability in SST, with temperatures decreasing from low to high latitudes. This gradient is represented by the colour scale ranging from red to green to blue, where red indicates warmer temperatures and blue represents cooler temperatures.

In addition to the latitudinal variability, the map shows the presence of coastal upwelling. The coastal upwelling is depicted by the blue colour, which extends from the

northeast coast towards the northwest, reaching the waters of CV and the surrounding areas. Coastal upwelling occurs when cold, nutrient-rich waters rise to the surface, influencing the local SST distribution. This upwelling contributes to the cooling of the coastal waters, leading to lower SST values along the affected regions.

The spatial distribution of SST, as shown in Figure 6a, impacts on the interannual variability of SST within the three boxes depicted in Figure 6b. The red box experiences higher temperatures than the other boxes.

On the other hand, the black box, which is influenced by coastal upwelling, exhibits the lowest temperatures among the three boxes. The upwelling brings cold to the surface, leading to cooler SST values in this region.

Regarding SST, the blue box has values in between the red and black boxes. Both latitude effects and the lesser impact of coastal upwelling influence its intermediate temperature range.

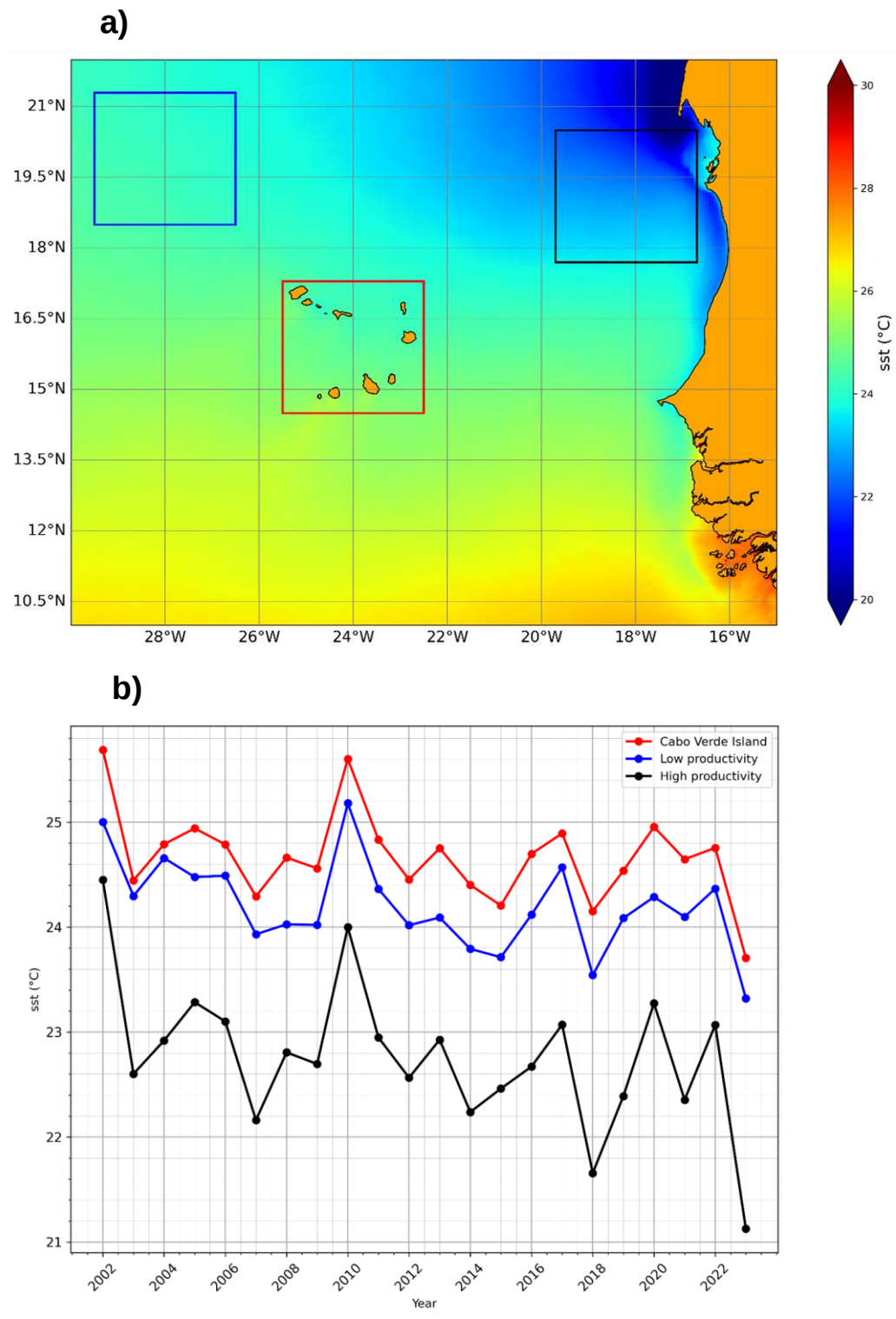

Figure 6: SST concentration variability around CV from Modis-Aqua satellite images. (a) Mean surface SST map from 2002 to 2022 over African coast including the CV Islands from Modis-Aqua product (in mg/m3). The three boxes (Black, red, blue) represent the various change in productivity. (b) Variability of mean SST surface values for the three boxes from 2002 to 2022 (the open ocean in blue curve, the CV in red curve and the near African coast in black curve).

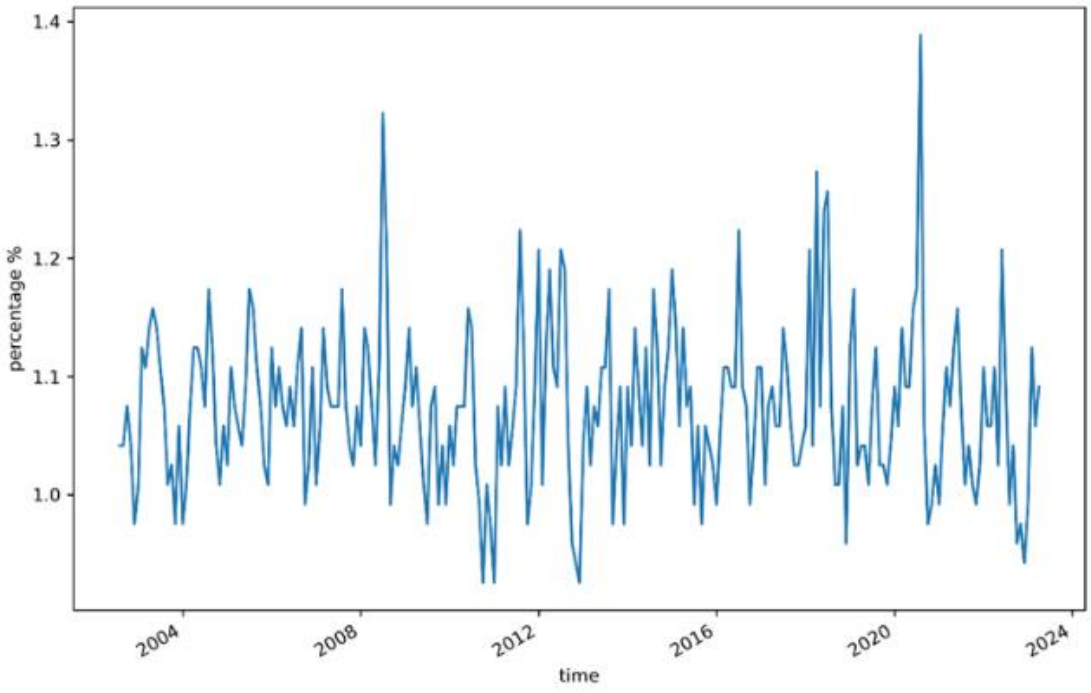

Figure 7: Percentage of missing value in the monthly SST satellite image from 2002 to 2022.

4.2. Local Variability of Chl-a and SST

4.2.1. Seasonal Variability of Chl-a and SST in Cabo Verde

The analysis provided insights into the seasonal variability of Chl-a and SST in CV, as depicted in Figure 8.

From the monthly climatologies, the results show that the maximum Chl-a values were recorded in January, reaching approximately 0.32 mg/m^3. In contrast, the minimum values were observed in August, with concentrations around 0.15 mg/m^3. This indicates a unimodal variability in Chl-a concentration, characterised by an increase during winter and Spring and a decrease during summer and Autumn.

SST also exhibits a unimodal pattern, with values increasing during summer and Autumn, reaching a high value in September at around 27 °C. Conversely, SST values generally decrease during winter and Spring, reaching a minimum value in March at approximately 23 °C. This delayed response of SST is due to the physical property of water, which reacts more slowly to heating than the atmosphere. The inverse relationship between SST and seasonal Chl-a might be explained by winter convection, which deepens the mixing layer and brings nutrients to the surface. Moreover, the advection of nutrient-rich water from

the Senegalese coast due to trade winds and the cooling effect in winter might further explain this inverse relationship.

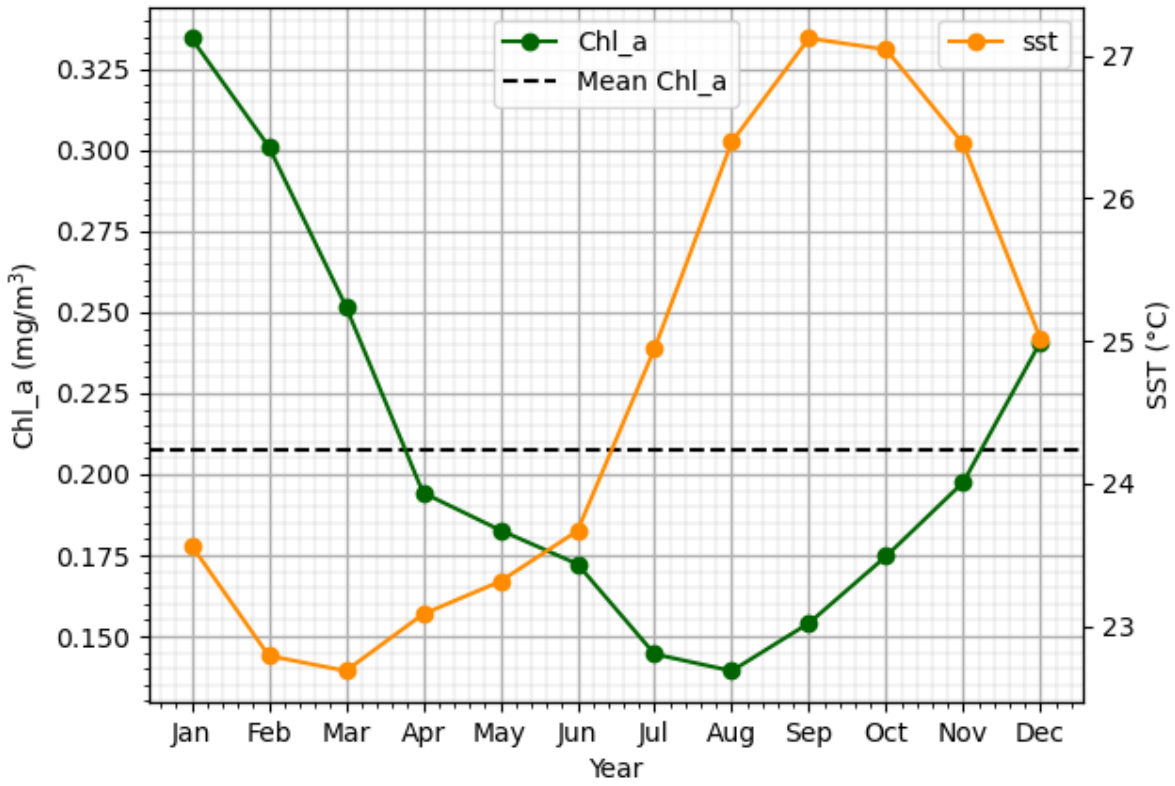

Figure 8: Seasonal variability of Chl-a and SST from Modis Aqua from 2003-2022 by surface monthly mean over CV, the green line represents the Chl-a seasonal variability and the orange line represents the SST seasonal variability and the black dashed line the mean Chl-a.

The monthly climatologies of surface Chl-a and SST, as illustrated in Figures 9 and 10, provide a visual representation of the inverse relationship observed in the seasonal variability of these two variables, as presented in Figure 8. Thus, Figure 9 presents a pronounced Chl-a signal during winter and spring, characterized by a prominent and widespread presence over CV in January. In contrast, the signal reduces considerably during summer and autumn. Figure 10, on the other hand, demonstrates an inverse situation compared to Figure 9 regarding SST.

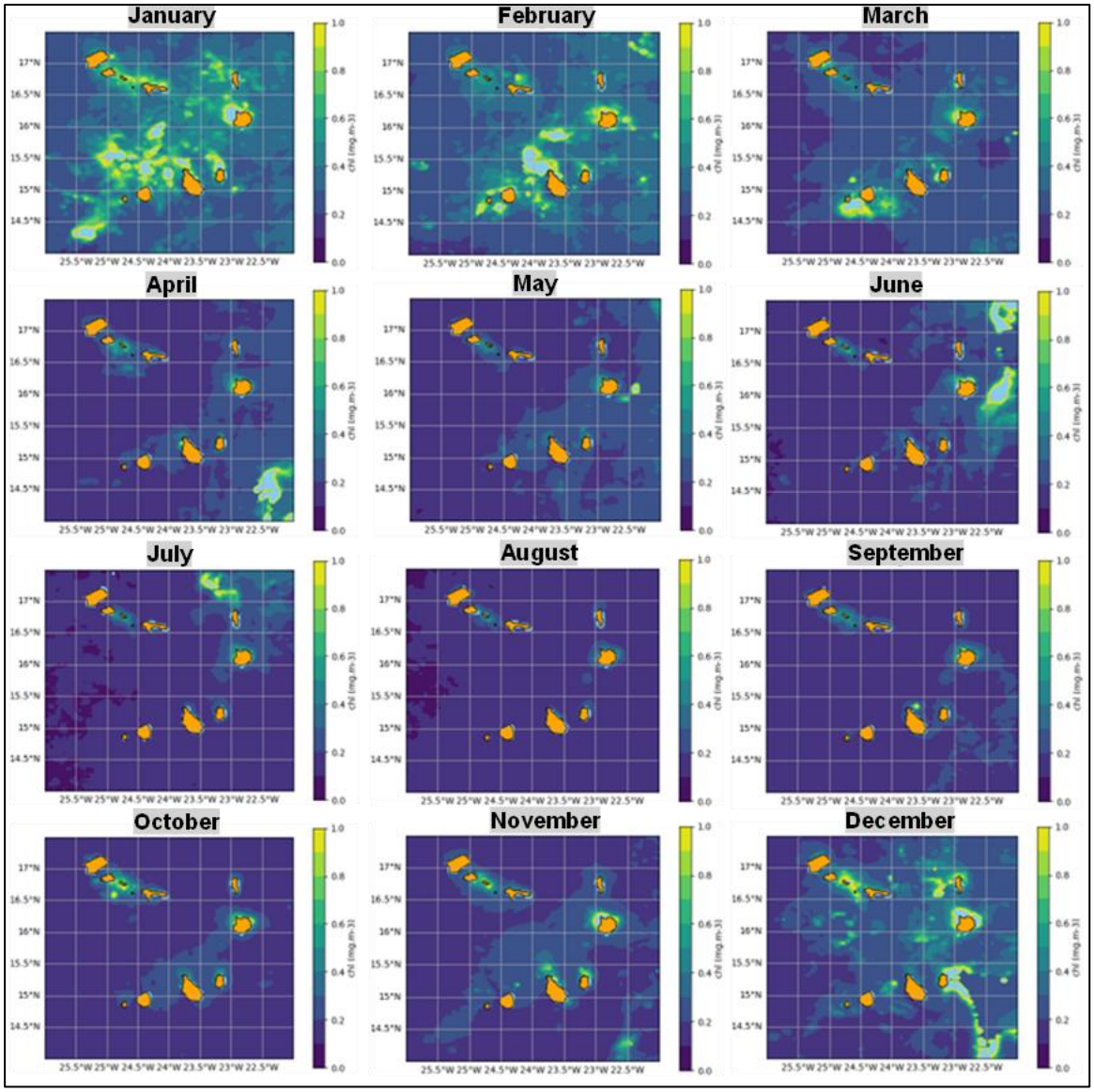

Figure 9: Monthly climatology of surface Chl-a 2002 to 2022 over CV Island from Modis-Aqua product (the values vary 0 to 1 mg/m^3 as shown the colour bar).

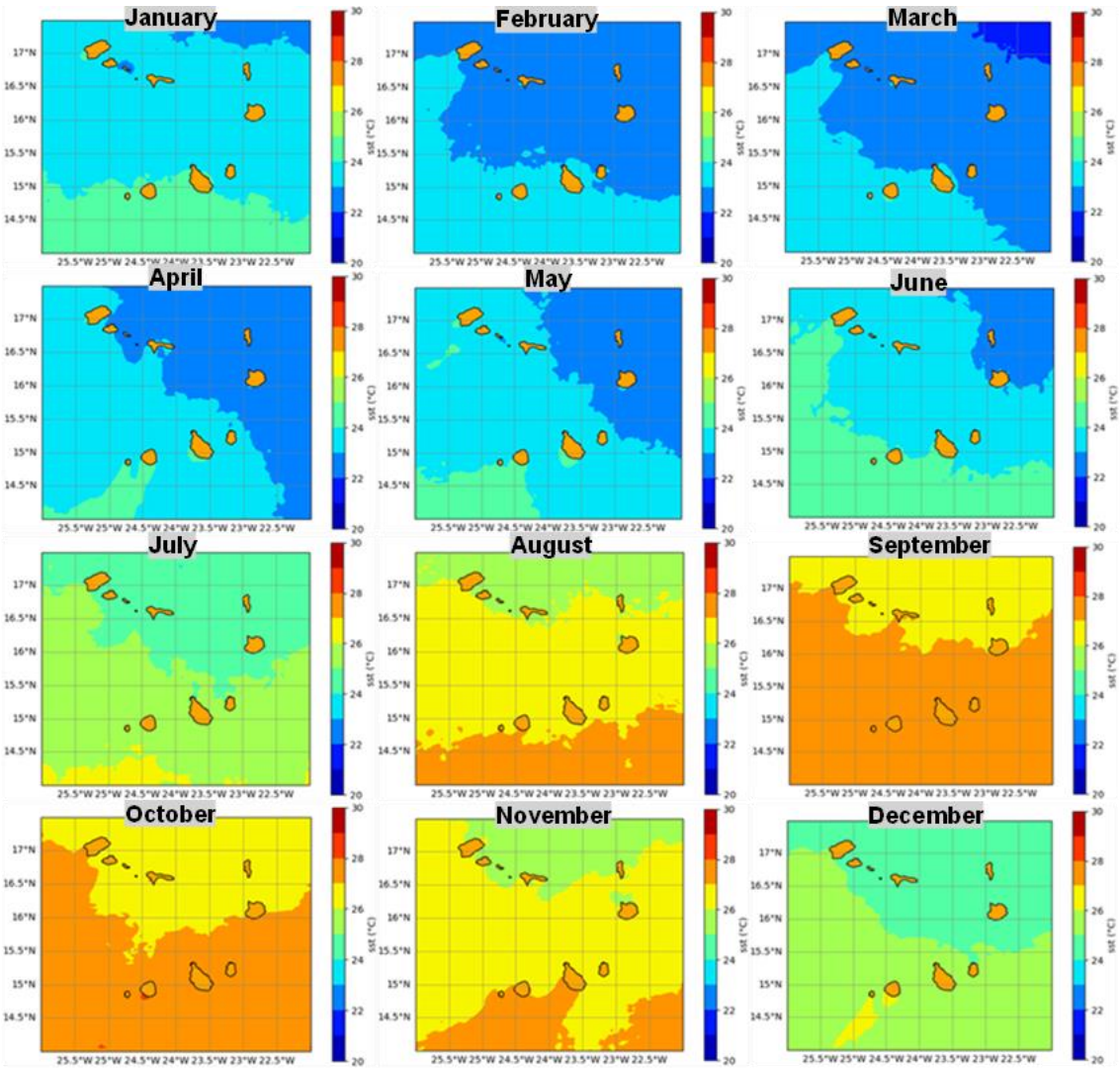

Figure 10: Monthly climatology of SST from 2002 to 2022 over CV Islands from Modis- Aqua product (the values vary 20 to 30 °C as shown the colour bar).

4.2.2. Seasonal Variability of Chl-a and SST around 6 different locations

Following the evaluation procedure for spatial and temporal productivity variability around the CV islands, Chl-a and SST were analysed at six locations, as shown in Figures 13 and 14. This examination provided valuable insights into the variations of Chl-a and SST across these specific areas.

Firstly, Chl-a were found to decrease progressively from the coast of the islands towards the open sea. Interestingly, a consistent seasonal pattern of Chl-a variability was observed at all six locations, with the variability becoming more pronounced as one moves away from the islands. The Chl-a ranged from 0.1 to 0.45 mg/m^3 (Figure 11b). Locations 1, 2, 3 and 4, closer to the northern region's islands, had higher Chl-a values (Figure 11b). Notably, Location 4, next to Boa Vista Island, notably recorded the most significant mean seasonal variability in Chl-a (Figure 11b). This corresponds effectively to the strong enrichment signal around Boa Vista Island observed in Figure 11b. In contrast, sites 5 and 6, located further south and further from the islands, had lower mean Chl-a values.

Secondly, the variability of SST at the six stations showed the same seasonal pattern with an increase in SST during the summer and a decrease in SST during the winter (Figure 12b). As shown in Figure 12b, stations 5 and 6 located at 14.5° N recorded the highest SST values compared to the four other locations. The SST ranged from 22 to 28 ° C (Figure 12b).

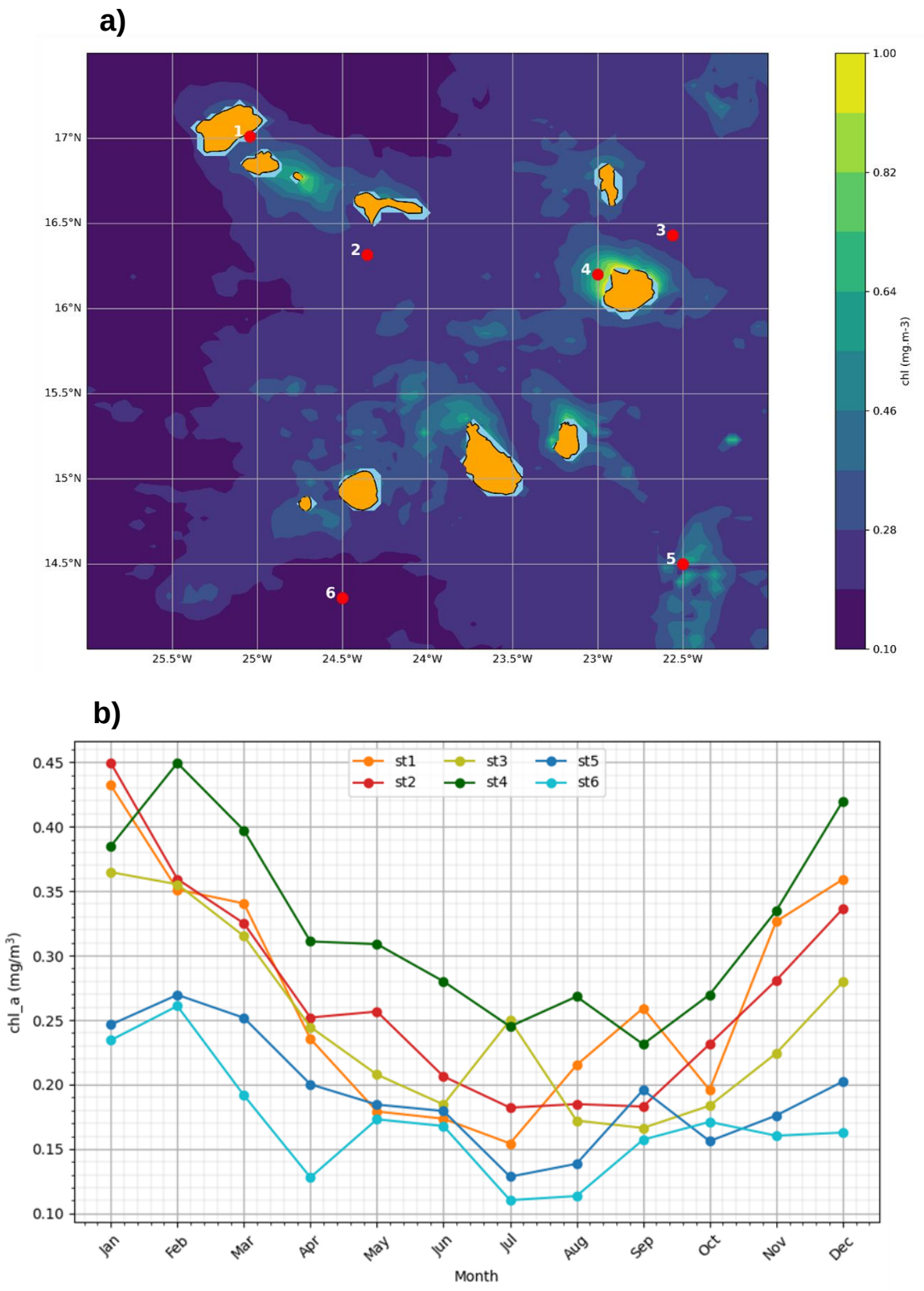

Figure 11: Chl concentration variability over CV Islands from Modis-Aqua satellite images with six (6) different locations identified in red dots. **(**a) Spatial distribution of mean surface Chl-a over CV with the red dot being the specific locations, (b) Seasonal variability of Chl-a in the 6 locations by surface monthly mean.

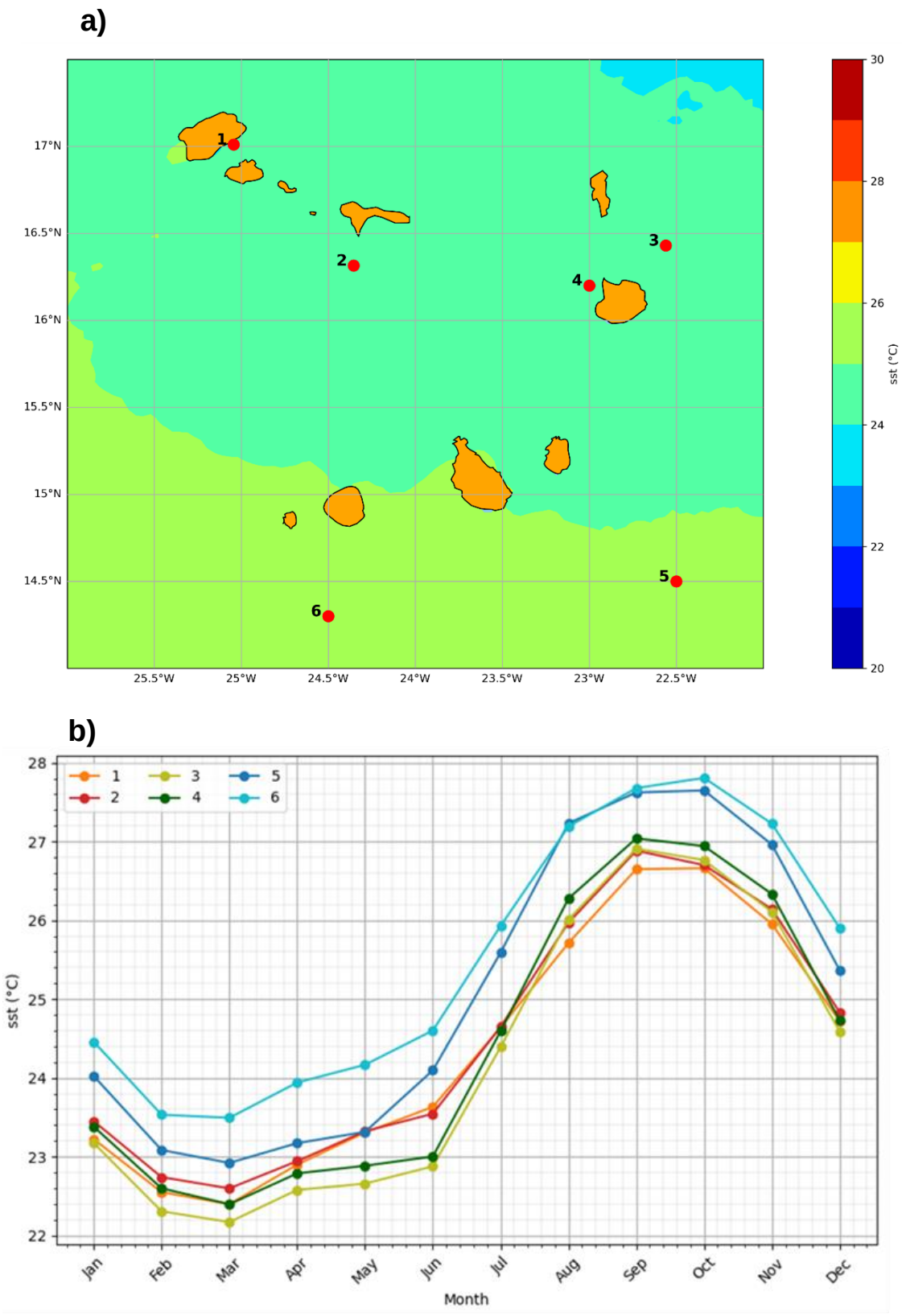

Figure 12: SST variability over CV Islands from Modis-Aqua satellite images with six (6) different locations identified in red dots. **(**a) Spatial distribution of mean surface SST over CV with the red dot being the specific locations, (b) Seasonal variability of SST in the 6 locations by surface monthly mean.

4.2.3. Interannual variability and regime shift of Chl-a and SST

The analysis of seasonal variability in Chl-a in CV identified anormal years in terms of Chl-a dynamics, specifically 2010, 2011, 2015, and 2018, as illustrated in Figure 13. These years stood out from the seasonal average in terms of Chl-a patterns. In particular, 2018 and 2015 exhibited Chl-a values above the seasonal average, while 2010 and 2011 had Chl-a values below the average. In particular, the years 2010 and 2018, with the Chl-a signals being much more pronounced in 2018 and less prominent in 2010 (Figure 14).

The distribution of Chl-a across all months was higher in 2018 and lower in 2010 compared to their respective seasonal averages. Notably, January 2018 displayed Chl-a values surpassing 0.5 mg/m^3.

Figure 15 depicts the seasonal distribution of SST in 2010 and 2018. In 2018, the SST was colder than the normal range from January and this trend continued until June. Conversely, in 2010, surface waters were warmer than usual, with a notable generation of warm waters observed in September.

The analysis of Figures 13, 14, and 15 reveals an interplay between Chl-a, SST, and their variation in 2010, 2011, 2015, and 2018. The elevated Chl-a levels in 2018 appear to align with the colder SST trend observed in the same year, while the warmer SST in 2010 correlates with reduced Chl-a.

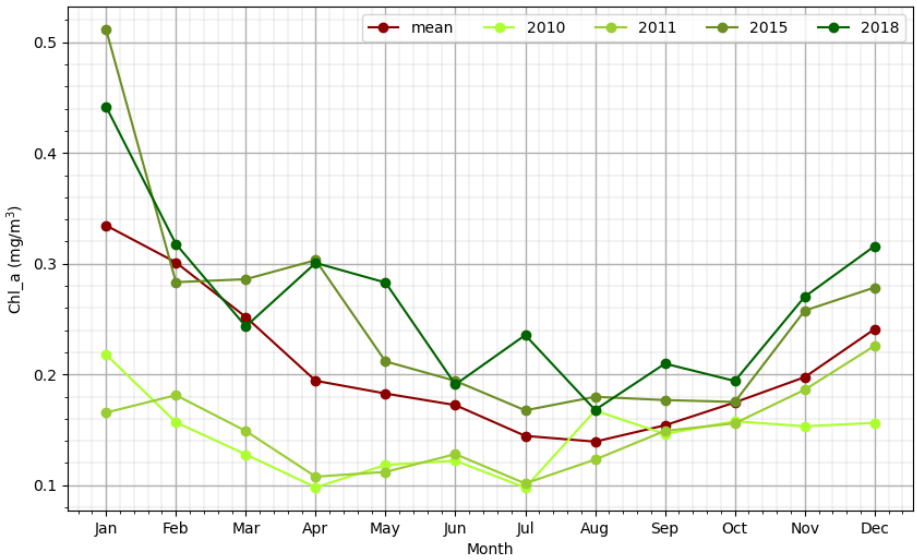

Figure 13: Seasonal variability of Chl-a from Modis-Aqua in CV for 2010, 2011, 2015, 2018 and mean (the green lines which change colour from dark to light represent respectively the years 2018, 2015, 2011 and 2010 and the red line is the mean).

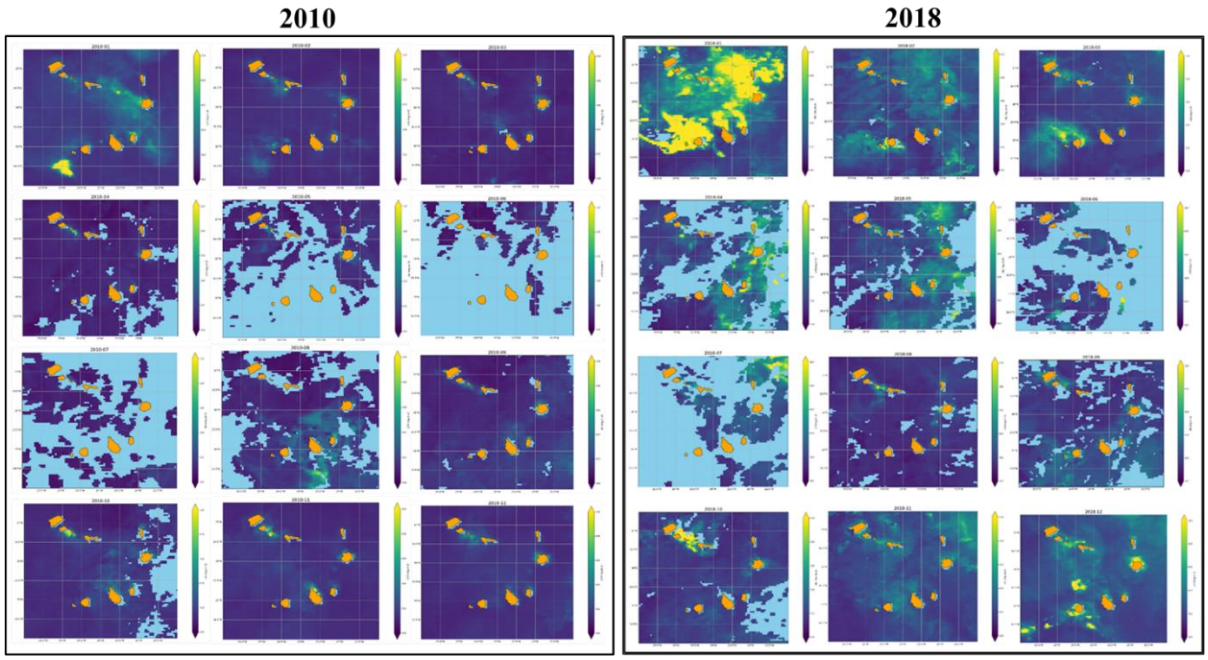

Figure 14: Mean surface Chl-a map of every month over CV Islands from Modis-Aqua product in 2010 and 2018.

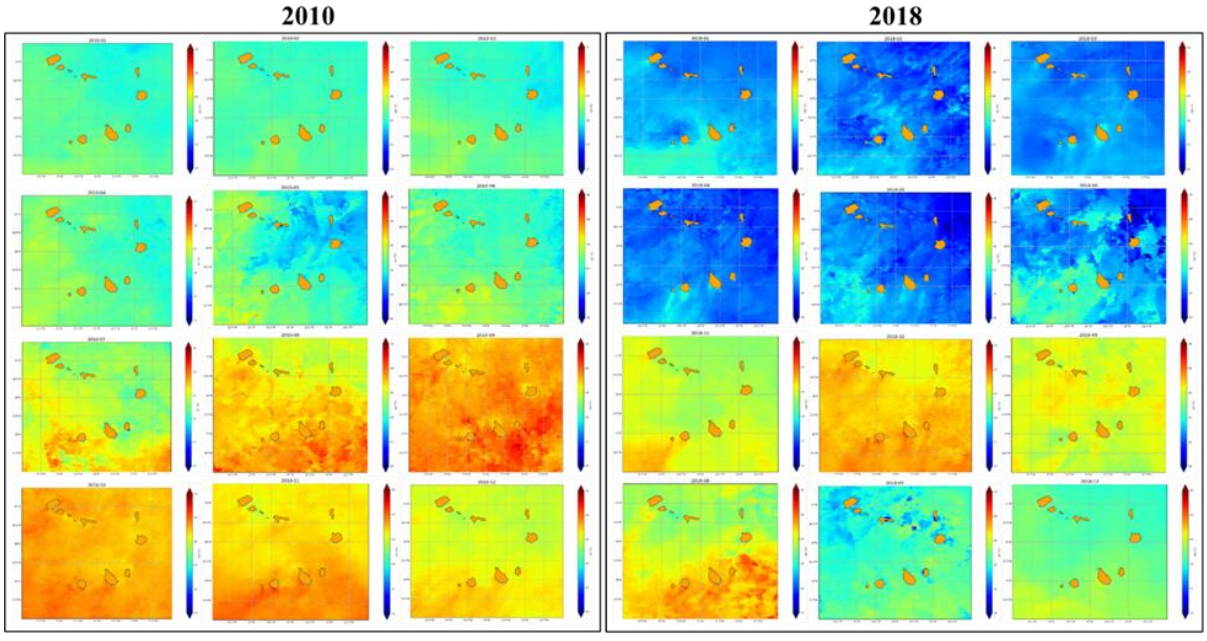

Figure 15: Mean surface SST map of every month over CV Islands from Modis-Aqua product in 2010 and 2018.

The analysis of interannual variability in Chl-a reveals a regime shift starting in 2013 (Figure 16). From this year onwards, the maximum and minimum values of Chl-a increased significantly, indicating an overall rise in Chl-a until 2022. Furthermore, 2010, 2011, 2015, and 2018 are part of a longer-term variability characterized by regime shifts.

Similarly, the interannual variability of SST identifies 2010, 2015, and 2018 as typical year with high average temperatures in 2010 (25.6 °C) and low SST values in 2015 and 2018 (24 °C). These years align with the anormal Chl-a variability. The trend analysis of Chl-a and SST 2002 to 2022 demonstrates an inverse relationship between these two variables. As SST increases, Chl-a tends to decrease.

Figure 17 presents the Hovmöller diagram depicting Chl-a and SST from 2003 to 2013 and from 2013 to 2022. The diagram reveals a consistent presence of Chl-a enrichment around the islands. The influence of coastal upwelling is also evident, influencing productivity in the waters of CV, as illustrated in the Chl-a Hovmöller diagram for 2018. The SST Hovmöller diagram demonstrates a relatively consistent interannual variability pattern.

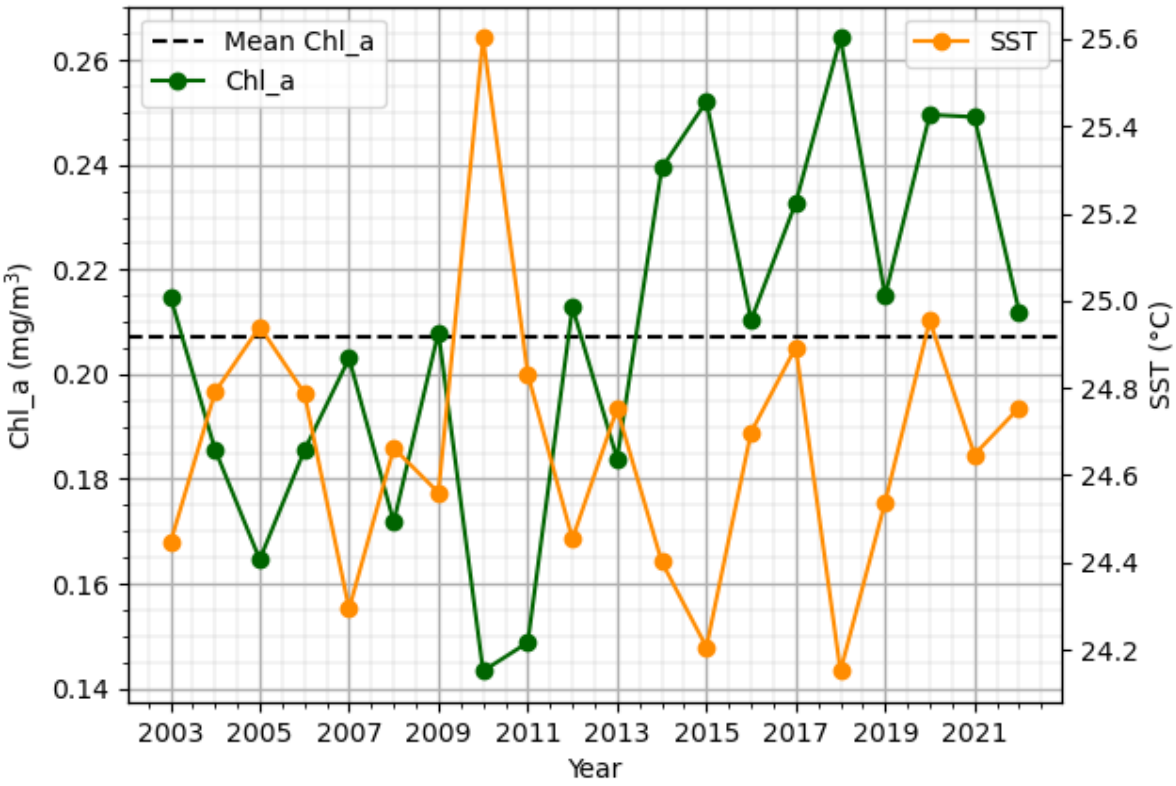

Figure 16: Interannual variability of SST and Chl-a from Modis-Aqua in CV from 2003-2022. The green line represents Chl-a interannual variability and the orange line represents SST interannual variability and the black dashed line the mean Chl-a.

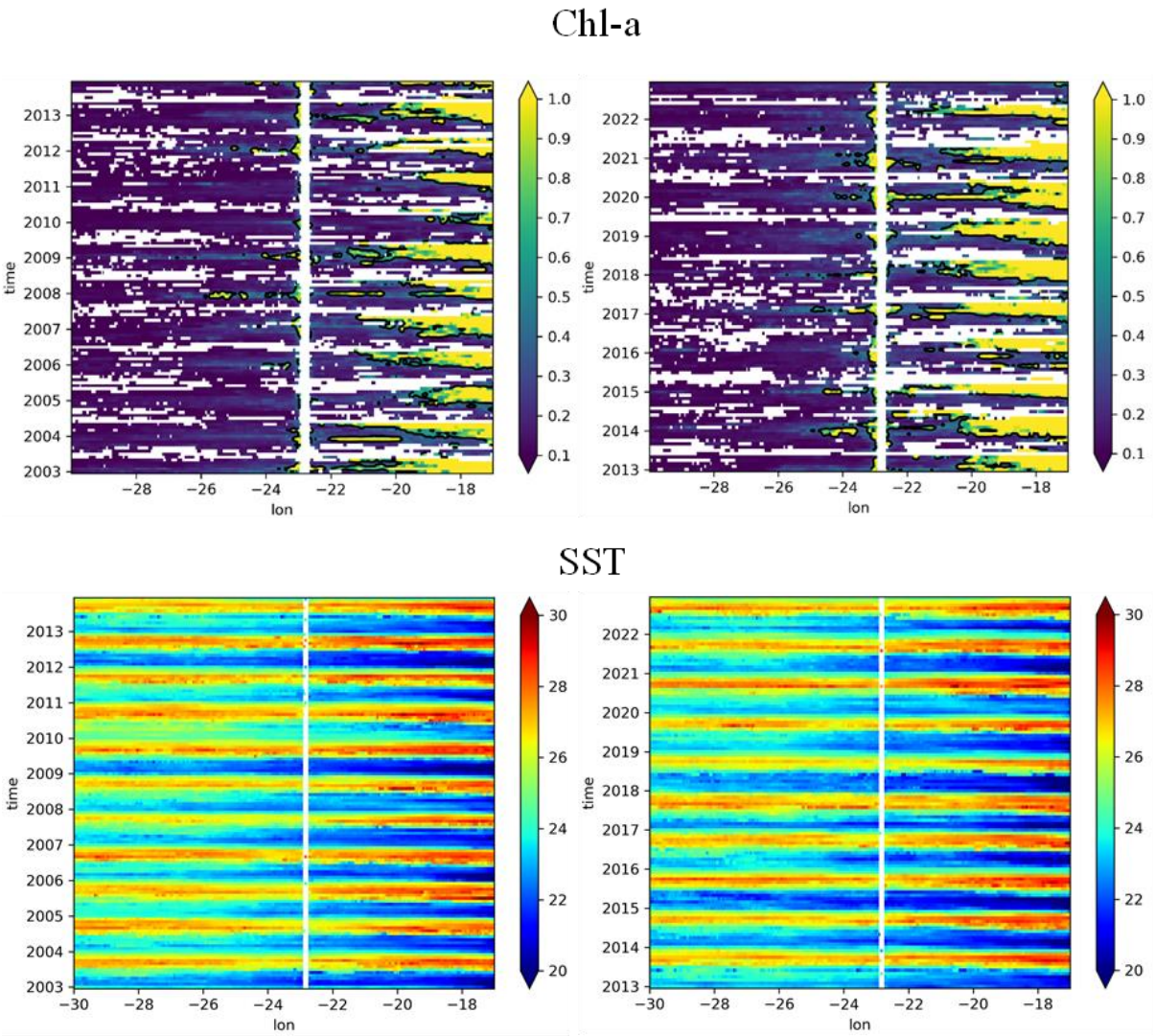

Figure 17: Hovmoller diagram of Chl-a and SST from 2003 to 2013 and 2013 to 2022 (the white line in the middle is CV islands).

4.2.4 Interannual variability of Chl-a and SST around 6 different locations

Figures 18 and 19 illustrate the interannual variability of Chl-a and SST at the six different locations. The patterns observed in the interannual variability of Chl-a are consistent with the seasonal variability of Chl-a at these locations (Figure 18). Locations 1, 2, 3, and 4, closer to the islands, exhibit higher annual average Chl-a than locations 5 and 6. This aligns with the general trend observed in the seasonal variability, where proximity to the islands contributes to higher Chl-a values. Conversely, locations 5 and 6, situated further away from the islands, record lower Chl-a. In addition, Figure 18 confirms the regime shift observed in Figure 16, but this time for all six stations.

Similarly, the interannual SST variability at the six locations follows the same pattern as the average SST values around CV (Figure 19). Additionally, locations 5 and 6 consistently demonstrate higher SST values than locations 1, 2, 3, and 4.

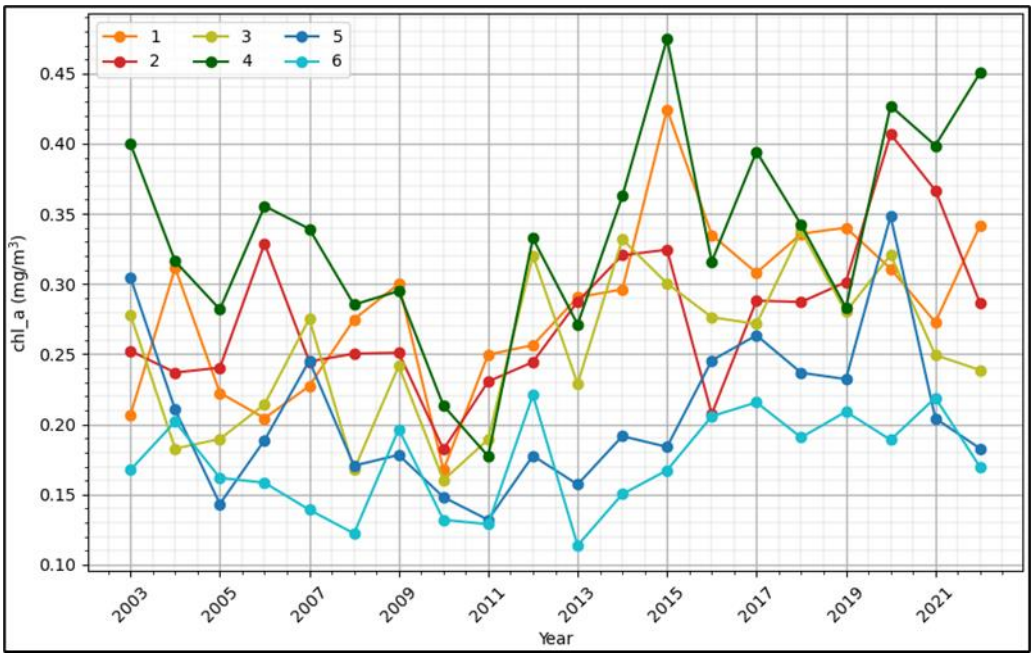

Figure 18: Interannual variability of Chl-a from Modis-Aqua in CV from 2003-2022 in the 6 locations.

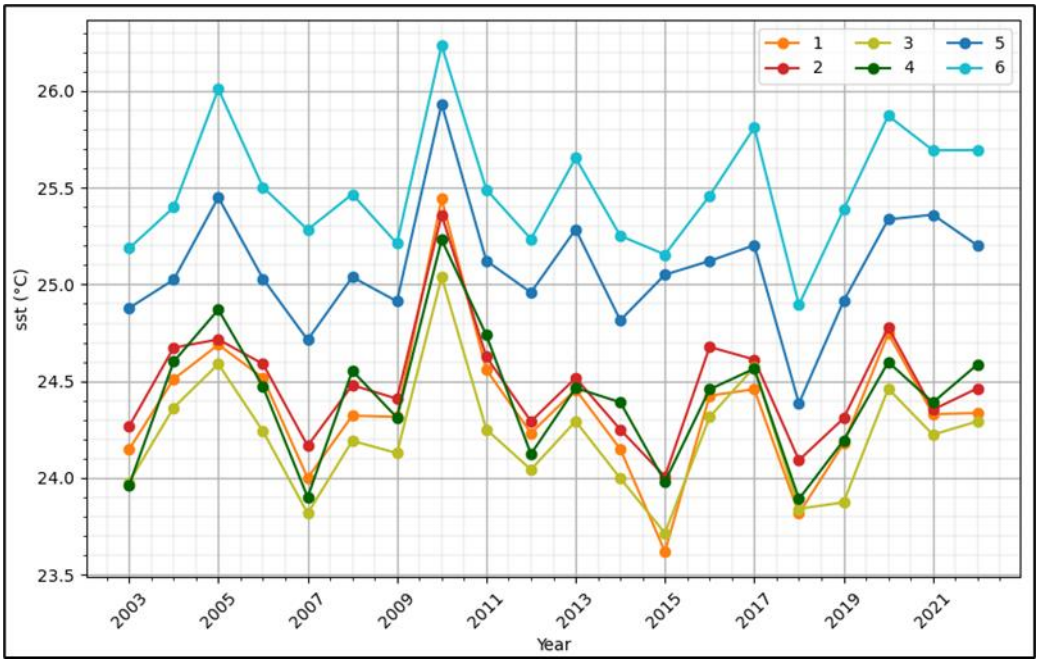

Figure 19: Interannual variability of SST from Modis-Aqua in CV from 2003-2022 in the 6 locations.

4.3. Trend analysis

The analysis of the Chl-a and SST time series from satellite data allowed for trend analysis over the entire dataset (Figure 20). Chl-a shows a relatively increasing trend (Figure 20a). However, the series shows significant interannual variability. Similarly, a relatively increasing trend is observed for SST (Figure 20b). Although there is no direct relationship between the variation in SST and Chl-a, however there is a similarity in the trend of the two series of dataset.

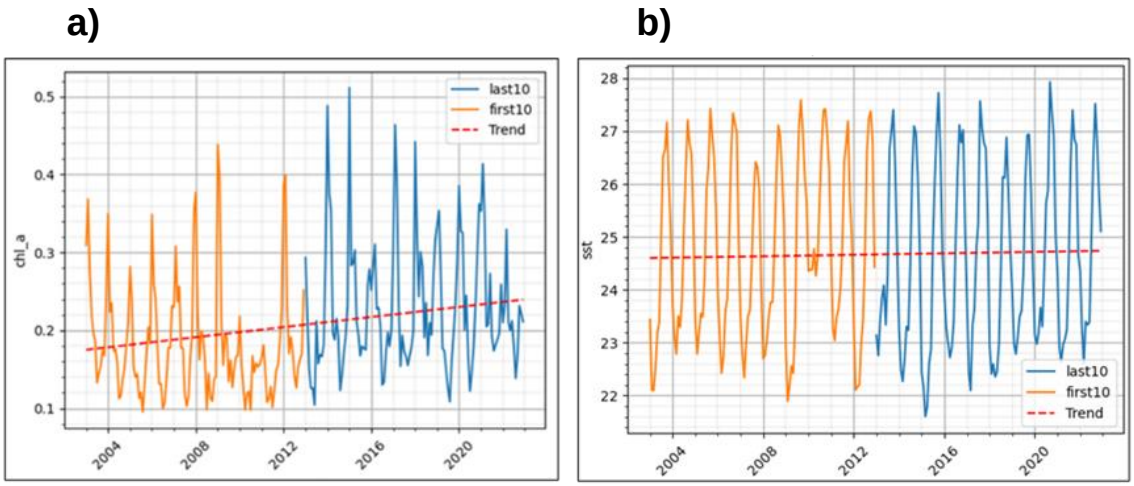

Figure 20: Trend analysis for Chl-a and SST from 2002 to 2022. (a) Mean monthly Chl-a (mg/m^3) with a linear regression fitted showing trend over CV from 2003-2022 from surface mean Chl-a Modis-Aqua satellite images. (b) Mean monthly SST (°C) with a linear regression fitted showing trend over CV from 2003-2022 from surface mean Chl-a Modis-Aqua satellite images. The orange line represents the time series from 2002 to 2013, the blue represents the time series from 2013 to 2022 and the dotted red line is the linear regression line.

4.4. Possible relationships between Chl-a variability and High Trophic Level

4.4.1. Interannual variability of Chl-a and total fisheries landing in Cabo Verde

The analysis of Chl-a variability and total fisheries landing in CV reveals a notable similarity in their patterns. High Chl-a years align well with years of large fish catches in CV, while low productivity years correspond to years of low fish catches. For example, the years 2015 and 2018, which were characterized by high fish catches, also exhibited high Chl-a as depicted the (Figure 21). Conversely, 2005, 2008, 2011, 2016, 2017, 2019, and 2020, marked by a decrease in fish catches, also displayed reduced Chl-a.

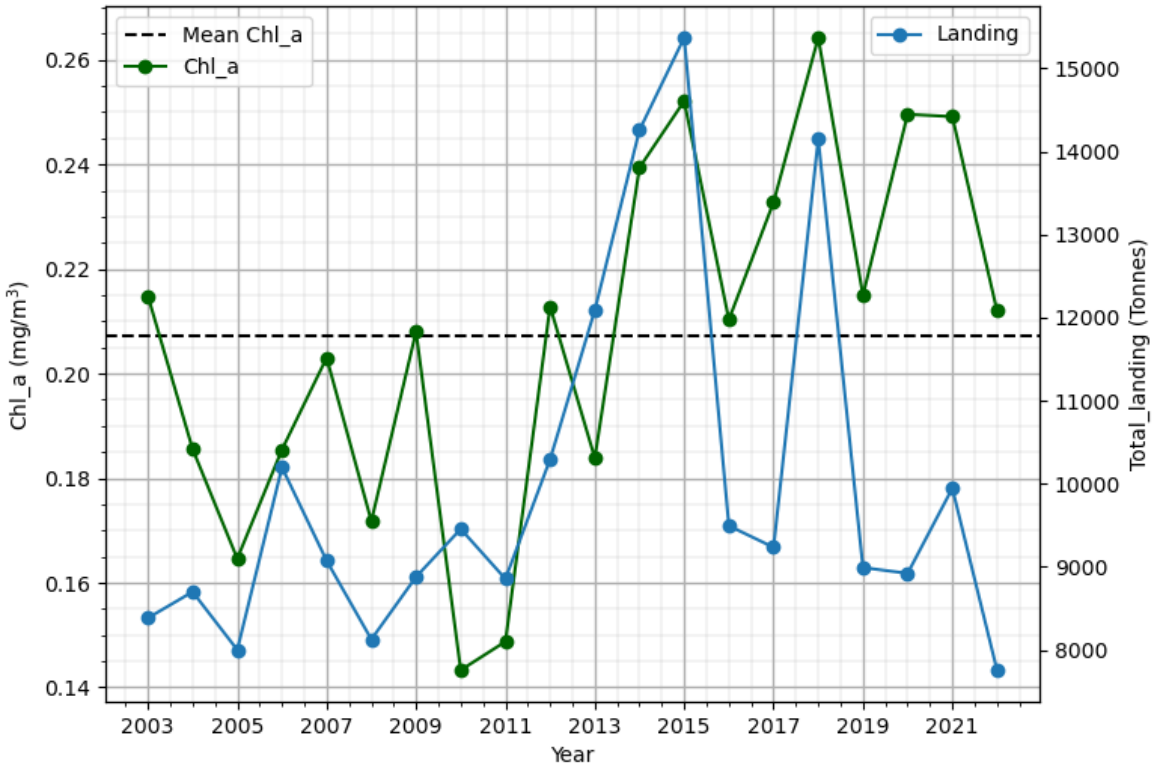

Figure 21: Interannual variability of Chl-a (mg/m^3) and Total fisheries landing (tonnes) in CV from 2003 to 2022. The green line represents the Chl-a, the blue line represents the Total landing and the black dashed line the mean Chl-a.

4.4.2. Chl-a and SST Variability and Small Pelagic Fish and Tuna

The relationships between Chl-a, SST variability, and the higher trophic levels were evaluated, focusing on small pelagic fish and tuna (Figure 22). Thus, a strong positive correlation was observed between Chl-a and the overall catch of small pelagic fish, showing a correlation coefficient 0.72 (Figure 22a). In addition, Figure 22b illustrated a moderate negative correlation between SST and the total catch of small pelagic fish, characterized by a correlation coefficient -0.49. Furthermore, Figure 22c showed also a strong positive correlation between Chl-a and the total tuna catch, yielding a correlation coefficient 0.78. Moreover, Figure 22d depicted a moderate negative correlation between SST and the total tuna catch, with a correlation coefficient -0.45. Overall, Chl-a had a stronger positive correlation with tuna and small fish catch than the SST which had moderate negative correlation. Also, a significant p-value less than 0.05 has been observed for all the correlations.

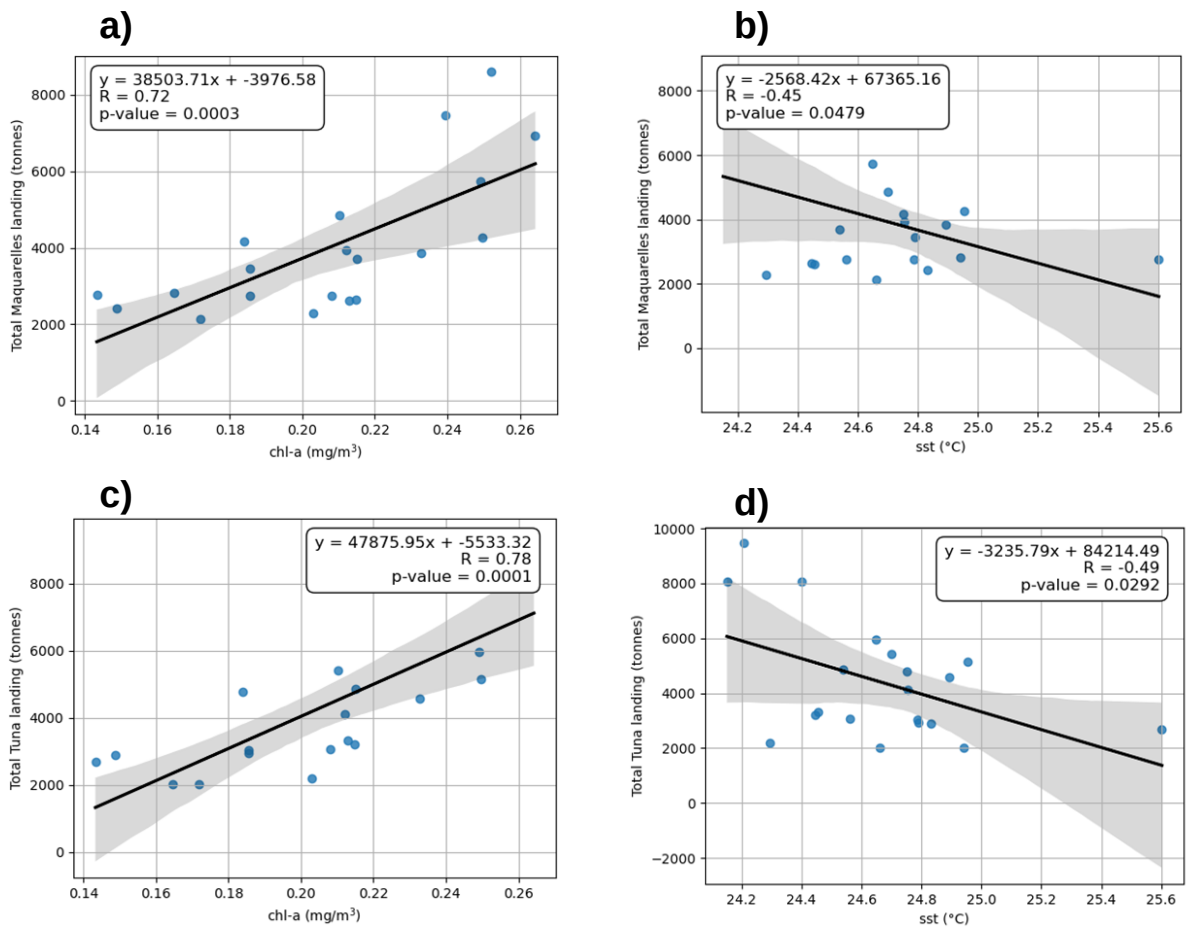

Figure 22: Correlation between Chl-a, SST, small pelagic fish, and Tuna total catch. (a) Correlation between Chl-a (mg/m^3) and total small pelagic fish landing (tonnes) in CV from 2003 to 2022. (b) Correlation between SST and total small pelagic fish landing (tonnes). (c) Correlation between Chl-a and the total tuna landing (tonnes). (d) Correlation between SST and the total tuna landing (tonnes). The blue dots are the correlation, the black line represents the regression line and the standard deviation is represented by the grey color, source: Modis Aqua Satellite image and IMar Data.

5. Discussion

5.1. Regional Variability of Chl-a and SST

The climatological map and time series of Chl-a and SST data provides insights into the spatio-temporal variability of phytoplankton biomass and its productivity in the study area (Figure 4 and 6).

The high concentration of Chl-a observed in the area within the black box (Figure 4), as compared to the other two areas of the red and the blue boxes, can be explained by its proximity to the Senegalese coast, which is characterized by the presence of coastal upwelling. This phenomenon is consistent with the findings in the Bohai Sea, where coastal enrichment of Chl-a is observed due to the upwelling of nutrient-rich water (Zhang et *al.,* 2017). Additionally, nutrient inputs from terrestrial runoff may contribute to the high enrichment of Chl-a in coastal waters, as seen in the study of the North Sea (McQuatters-Gollop et *al*., 2007).

Conversely, the blue box, located far from the coast and lacking intensive mixing processes, exhibits negligible Chl-a concentrations. Without sufficient nutrient supply, phytoplankton productivity is limited, leading to low Chl-a concentrations.

The red box exhibits intermediate Chl-a concentrations and can be attributed to the IME and the associated oceanic physical processes. Islands can create localized hydrodynamic features that enhance primary productivity (Falco et *al.,* 2022). These features include the upwelling of nutrient-rich deep waters to the surface, eddies that concentrate nutrients and organic matter, and turbulence and mixing that promote nutrient exchange. In addition, islands can form fronts and convergence zones and provide sheltered areas, helping to increase primary productivity and support diverse marine ecosystems.

The observed spatial distribution of SST and its possible influence on Chl-a align with previous studies on productivity in upwelling areas. Coastal upwelling is known to enhance productivity in marine ecosystems, and such upwelling is evident in the SST patterns observed in the study area. This aligns with the findings of Minas et *al.* (1986) that highlight the relationship between upwelling and increased productivity.

The influence of warm equatorial waters on the study area's SST distribution also aligns with previous research (Ramos et *al.,* 2012). Proximity to the equatorial region exposes the study area to higher solar radiation, contributing to warmer SST. The input of warm equatorial waters further influences the SST distribution, affecting the distribution of Chl-a.

Furthermore, the percentage of missing values for Chl-a and SST (Figure 5 and 7) displays a divergent pattern. While Chl-a data exhibit significant missing values, particularly during certain seasons like summer, SST data demonstrate lower instances of missing values. The substantial absence of data in the Chl-a images can be attributed to sensor-related challenges and the presence of clouds over CV, especially during summer. This data deficiency has been mentioned in various studies, including Cardoso et *al*.'s work in 2020. Nonetheless, satellite imagery remains an essential tool for Chl-a estimation. The Modis Aqua satellite images used in this study have been extensively validated due to their suitable spatial resolution, prolonged temporal coverage, validation against in-situ measurements, and widespread use in scientific research (Wang et *al.,* 2015; Li et *al.*, 2017; Hu et *al.*, 2012; Cardoso et *al.*, 2020). This affirms its value for analysing Chl-a variability in marine ecosystems.

5.2. Local Variability of Chl-a and SST

The analysis reveals a distinct seasonal pattern in Chl-a and SST at CV. The Chl-a shows a unimodal variability, with maximum values in winter and minimum values in summer. Similarly, SST follows a unimodal pattern, with higher temperatures observed in summer and lower temperatures in winter (Figure 8). According to studies conducted in the regions by Pradhan et *al.* (2006), the enrichment during winter has been explained by two processes that have a coherent relationship between SST and Chl-a, namely convection and advection from upwelling. The presence of Sahara dust in winter also increases nutrients. And so, one might question whether this inverse relationship between Chl-a and SST are linked to more significant winter convection or the influx of waters through advection from the Senegalese upwelling. However, based on the SST maps, this influence might be regional, suggesting that upwelling occurs more sporadically.

In general, SST appears to be distributed according to latitude and longitude (Figure 10). However, they appear to be strongly influenced, possibly by the surface currents that carry the cold, nutrient-rich coastal waters back to CV from January to June. In contrast, the second phase which runs mainly from August to November, is characterised by warmer temperatures that the high solar radiation can explain.

Analysis of variability in Chl-a and SST at the six sites provides valuable information on these parameters' spatial and seasonal dynamics (Figure 11 and 12). The observed decrease in Chl-a from coastal areas to the open sea suggests a decreased gradient in phytoplankton

biomass (Figure 11). The stations (1, 2, 3 and 4, Figure 11) closest to the islands had higher Chl-a values. In contrast, the more remote sites (5 and 6) had lower Chl-a.

A hypothesis can be formulated that this enrichment near the islands is a result of IME (nutrient availability, water mixing processes, and the influence of local environmental factors such as rainfall). Islands can favor nutrient enrichment through local upwelling phenomena or by acting as sources of nutrients from terrestrial run-off. These favorable conditions encourage phytoplankton growth and lead to high levels of Chl-a. It is possible that sites (5 and 6) do not benefit as much from the influence of the islands in terms of nutrient input and mixing processes. The lower Chl-a in these locations could be the result of limited access to nutrient-rich waters and environmental conditions that are less favorable to phytoplankton growth. However, this remains a hypothesis that needs to be verified.

The seasonal trends observed in figures 18 & 19 for SST align with those for Chl-a, indicating a close relationship between the two parameters. Figure 18 validates the identified shift in regime as shown in Figure 16, extending this observation to all six stations. The fact that stations 5 and 6, located further south, recorded the highest SST values can be attributed to the effects of latitudinal solar radiation.

Analysis of abnormal years in terms of Chl-a in CV provides insight into significant deviations from the seasonal average. It highlights the dynamic nature of phytoplankton biomass in the region. The years 2010, 2011, 2015, and 2018 are anomalous years with distinct Chl-a patterns (Figure 13).

In 2018 and 2015, higher concentrations of Chl-a were observed compared with the seasonal average. The higher Chl-a values suggest a high availability of nutrients and increased biological activity and also climate change. These years can be periods of increased productivity, potentially indicating favorable conditions for phytoplankton growth likely due to the strengthening of surface currents that have brought back rich coastal waters in these years. This remains a hypothesis since it was demonstrated in this work.

On the other hand, 2010 and 2011 exhibited lower Chl-a concentrations compared to the seasonal average. These years may have experienced environmental conditions that limited phytoplankton growth, such as reduced nutrient availability or weakening of the surface current.

A notable difference between January 2018 and January 2010 is the enrichment of the Chl-a observed in January 2018. This indicates a substantial increase in phytoplankton biomass during this specific month compared with January 2010.

Furthermore, SST patterns in 2010 and 2018 diverged. In 2018, colder than normal temperatures were observed from January to June, indicating a potential influence on the Chl-a enrichment observed during this period. In contrast, 2010 experienced a generation of warm waters in September, which may have contributed to the lower Chl-a concentrations observed that year.

Overall, the analysis highlights the importance of local factors such as proximity to islands shaping spatial and seasonal variability in Chl-a and SST in CV. In addition, expected years of Chl-a and the corresponding SST patterns highlight the interaction between environmental factors and biological productivity in CV. These results highlight the importance of considering physical and biological processes when studying the dynamics of marine ecosystems.

Furthermore, analysis of the interannual variability of Chl-a reveals a significant change in the Chl-a regime from 2013 onwards, with a steady increase in Chl-a values over time (Figure 16). Among the years examined, 2010, 2011, 2015 and 2018 are standard years with notable variability in Chl-a. Remarkably, these fluctuations correspond to changes in Chl-a and exhibit similar variability as observed in SST. Trend analysis further highlights the inverse relationship between Chl-a and SST. As SST increases, Chl-a tends to decrease, and vice versa. This leads to the hypothesis that the variability in SST could potentially serve as a proxy for identifying processes such as convection and advection, which might impact phytoplankton growth and Chl-a dynamics in the study area. And also, the regime shift might be explained by the environmental change in the regions which still need to be demonstrated.

Hovmöller diagrams provide further evidence of Chl-a enrichment around CV Archipelago. These diagrams illustrate the temporal and spatial patterns of Chl-a and SST, highlighting areas of higher productivity and the influence of physical processes.

The islands' proximity plays an important role in the evolution of Chl-a. These results are in line with observations of seasonal variability, further reinforcing the influence of proximity to islands on Chl-a and SST. The presence of coastal upwelling, and nutrient-rich water near the islands contributes to higher Chl-a. Overall, the consistent patterns observed in both the interannual and seasonal variability of Chl-a and SST underline the strength of these

relationships on different time scales and in different locations. Proximity to islands appears to be a key factor in variability in Chl-a and SST.

5.3. Trend analysis

The trend analysis reveals an upward trend in both Chl-a and SST from 2003 to 2022 (Figure 20). Although there is no direct link between the variation in SST and Chl-a, a similarity in the trend displayed by both data series can be observed. This result appears to contrast with the study by Boyce et *al.* (2010), which reported a global decline in phytoplankton biomass, and those of Lathuilière et *al.* (2008). It should be noted that Lathuilière et *al.* (2008) identified a large-scale decrease in Chl-a around CV based on SeaWiFS data from 1992 to 2005. However, global observations might not necessarily align with regional observations due to the presence of the CV islands, which can create specific conditions.

Moreover, it is important to note that the findings of Lathuilière et *al.* (2008) are inconsistent with those of the present study, and the sensors used are not the same. Therefore, the hypothesis that can be proposed considering the slightly increasing trend in Chl-a and SST is related to an environmental change, which could potentially be confirmed by the regime shift discussed further. Additionally, it should be emphasized that there is pronounced interannual variability at the endpoints of the series, which could impact the observed trend.

5.4. Chl-a Variability and High Trophic Level

The analysis of Chl-a and total landings from the CV fishery reveals a consistent pattern (Figure 21). Years of high Chl-a correspond to years of high fish catches, indicating a possible close link between phytoplankton abundance and fish populations. Increased primary production, facilitated by a distinctive input of nutrients such as upwelling and nitrogen fixation, contributes to increased fish resources around the islands (Shiozaki et *al.,* 2014). Conversely, years of low Chl-a correspond to a reduction in fish catches, suggesting less favourable conditions for phytoplankton, and possibly zooplankton growth and subsequent impacts on fish populations. The decline in fish landings observed from 2019 onwards further suggest the link between Chl-a variability and fishing dynamics.

The positive correlation between Chl-a and the catch of small pelagic fish in CV supports the results of Li et *al.* (2014), who studied the distribution of chub mackerel in Chinese coastal waters. Their study aligns with the positive correlation observed in CV, suggesting the role of Chl-a in supporting prey availability for small pelagic fish. The negative correlation between SST and tuna catch in CV is consistent with research conducted by Erauskin-

Extramiana et al. (2019) and Andrade & Garcia (1999). These two studies confirm the negative correlation observed in CV, indicating that SST variability can influence tuna distribution and availability.

Chl-a depicted a strong correlation with fish landings, whereas SST showed a moderate correlation (Figure 22). This supports the idea that Chl-a serves as a proxy for primary production. Furthermore, fishing pressure can also vary from year to year, depending on changing demands that may increase or decrease. The question of fishing pressure is evident in the decrease in fishing dataset in 2019 and 2020, hypothesized to be due to the COVID-19 pandemic. Establishing a link between Chl-a and fisheries data can pose problems because Chl-a is an indicator of primary productivity, and its direct influence on the upper marine food chain involves initial interactions with zooplankton. Moreover, Chl-a is considered according to Friedland et *al.* (2012), like an indicator of energy transfer from primary producers like phytoplankton to higher trophic levels and ultimately to fishery yields.

In this study I focused on the spatio-temporal variability of Chl-a and SST. By regulating nutrient availability SST highlights the influence of ocean dynamics in shaping Chl-a and possible marine ecosystem dynamics in CV. Considering their significance as essential indicators of phytoplankton abundance and environmental conditions, wind speed, precipitation, Aerosol Optical Depth, PAR, and CDOM should be considered for further study in exploring the driving mechanisms in Chl-a variability in CV. Furthermore, biogeochemical models can also offer data that can complement and validate satellite observations, providing a more complete understanding of Chl-a dynamics. However, due to the time constraints of this particular study, we have chosen to focus on Chl-a and SST ocean colour remote sensing data from Modis-Aqua. In addition, although available daily, meteorological data on wind speed and precipitation can be combined with daily satellite data to study the daily variability of Chl-a in the CV region. This integration will allow a more detailed examination of short-term fluctuations in Chl-a and its relationship with meteorological conditions.

6. Conclusion

Analysis of climatological maps and time series data of Chl-a and SST provides insights into the spatio-temporal variability at regional level. And so, the region within the black box exhibits higher Chl-a concentrations compared to the red and blue boxes, along with lower SST. The hypothesis put forward is due to its proximity to the Senegalese upwelling. This phenomenon finds support in similar findings in other regions such as the Bohai Sea. The blue box, situated far from the coast, displays minimal Chl-a concentrations along with relatively warm SST. This could be due to potential limitations in convections and advections from the Senegalese coast. In addition, the red box shows intermediate Chl-a concentrations and relatively warm SST. This could possibly be attributed to the presence of islands, which give rise to the phenomenon known as IME. The fact that the red box is located in the warmer low latitudes and closer to the equator than the other two boxes is hypothesized to explain its higher SST.

Moreover, the percentage of missing values for Chl-a and SST data exhibits a divergent pattern. Chl-a data have more missing values, especially during certain seasons like summer. This is linked to potential sensor issues and the seasonal presence of dust over Cabo Verde. Despite this, satellite images, particularly Modis Aqua images, remain valuable for Chl-a estimation, given their extensive validation against in-situ measurements and their widespread use in scientific research.

Variabilities are evident in both Chl-a and SST, revealing their inverse seasonal and interannual relationship. This connection has been explained by the possible intensification of winter convection or the advection of water from the Senegalese upwelling. Chl-a and SST analysis across six sites shows spatial and seasonal dynamics, with decreasing Chl-a from coastal to offshore areas, possibly due to limited nutrient access at remote sites. SST trends match Chl-a, including a change in regime. In addition, from 2013 onwards, a regime shift has been observed. Also, anomalous Chl-a years (2010, 2011, 2015, 2018) deviate from seasonal patterns, has been observed, with 2018 and 2015 indicating favorable conditions for phytoplankton growth due to stronger surface currents, while 2010 and 2011 exhibit lower Chl-a likely due to environmental constraints. These results underline the dynamic nature of Chl-a and highlight the importance of understanding regional variability in the context of global trends.

Finally, a notable change in Chl-a dynamics has been observed over the last decade around CV. The upward trend from 2003 to 2022 of Chl-a and SST indicates a possible relationship between SST and Chl-a. Chl-a depicted a strong correlation with fish landings, whereas SST showed a moderate correlation.

A relationship between SST and Chl-a variability has been found, indicating that SST is linked to processes involved in the phytoplankton biomass variability. Warmer SST conditions result in lower Chl-a while colder SST conditions favor higher Chl-a. And so, warm conditions cause stratification with block vertical mixing. On the other hand, cold water promotes the deepening of the thermocline and the availability of nutrients at the surface which is good for marine organisms.

These results underline the need to continue monitoring efforts and highlight the complex interactions between environmental factors, Chl-a, SST, and fish populations. Implementing sustainable fishing practices and preserving fishery resources in CV requires a comprehensive understanding of these relationships. Further research is needed to study the factors behind these changes and their implications for marine ecosystems and biogeochemical cycles.

7. Recommendations

The results of this study highlight the crucial need for continuous monitoring of Chl-a and SST in CV. Monitoring of these environmental factors is essential for fisheries managers and conservationists to obtain valuable information on the productivity and distribution of fish species in the region. This knowledge can inform decision-making processes and support the implementation of sustainable fishing practices.

Collaboration with research institutions and organizations is strongly encouraged to improve data, analysis and interpretation. By encouraging such collaboration, it is possible to better understand the complex interactions between environmental factors, phytoplankton biomass and productivity and fish populations in CV.

Another essential aspect is raising public awareness of the importance of monitoring Chl-a concentrations and SST for sustainable fisheries management. Educating local communities, fishermen and stakeholders about the benefits of monitoring and how it contributes to the long-term health and productivity of marine ecosystems is essential.

In addition, it is essential to continually evaluate and adapt fisheries management strategies based on the lessons learned from observations. This adaptive management approach will allow adjustments to be made in response to changing environmental conditions, thereby ensuring the effectiveness of conservation and management efforts in improving phytoplankton growth.

By implementing these recommendations, CV can improve its fisheries management and conservation practices, leading to sustainable fishing and preserving of its valuable marine resources.

8. References

Andrade, H. A., & Garcia, C. A. E. (1999). Skipjack tuna fishery in relation to sea surface temperature off the southern Brazilian coast. *Fisheries Oceanography*, *8*(4), 245–254. https://doi.org/10.1046/j.1365-2419.1999.00107.x

Andrade, I., Sangrà, P., Hormazabal, S., & Correa-ramirez, M. (2014). Deep-Sea Research I Island mass effect in the Juan Fernández Archipelago (33 1 S), Southeastern Paci fi c. *Deep-Sea Research Part I*, *84*, 86–99. https://doi.org/10.1016/j.dsr.2013.10.009

Behrenfeld, M. J., & Falkowski, P. G. (1997). Photosynthetic rates derived from satellite-based chlorophyll concentration. *Limnology and Oceanography*, *42*(1), 1–20. https://doi.org/10.4319/lo.1997.42.1.0001

Behrenfeld, M. J., O'Malley, R. T., Siegel, D. A., McClain, C. R., Sarmiento, J. L., Feldman, G. C., Milligan, A. J., Falkowski, P. G., Letelier, R. M., & Boss, E. S. (2006). Climate-driven trends in contemporary ocean productivity. *Nature*, *444*(7120), 752–755. https://doi.org/10.1038/nature05317

Boyce, D. G., Lewis, M. R., & Worm, B. (2010). Global phytoplankton decline over the past century. *Nature*, *466*(7306), 591–596. https://doi.org/10.1038/nature09268

Caldeira, R. M. A., Groom, S., Miller, P., Pilgrim, D., & Nezlin, N. P. (2002). Sea-surface signatures of the island mass effect phenomena around Madeira Island, Northeast Atlantic. *Remote Sensing of Environment*, *80*(2), 336–360. https://doi.org/10.1016/S0034-4257(01)00316-9

Cardoso, C., Caldeira, R. M. A., Relvas, P., & Stegner, A. (2020). Islands as eddy transformation and generation hotspots: Cabo Verde case study. *Progress in Oceanography*, *184*(January), 102271. https://doi.org/10.1016/j.pocean.2020.102271

Cassianides, A., Martinez, E., Maes, C., Carton, X., & Gorgues, T. (2020). Monitoring the influence of the mesoscale ocean dynamics on phytoplanktonic plumes around the Marquesas Islands using multi-satellite missions. *Remote Sensing*, *12*(16). https://doi.org/10.3390/RS12162520

Chavez, F. P., Messié, M., & Pennington, J. T. (2011). Marine primary production in relation to climate variability and change. *Annual Review of Marine Science*, *3*, 227–260. https://doi.org/10.1146/annurev.marine.010908.163917

Dierssen, H. M., & Randolph, K. (2012). Encyclopedia of Sustainability Science and Technology. In *Encyclopedia of Sustainability Science and Technology*. https://doi.org/10.1007/978-1-4419-0851-3

Doty, M. S., & Oguri, M. (1956). The island mass effect. *ICES Journal of Marine Science*, *22*(1), 33–37. https://doi.org/10.1093/icesjms/22.1.33

Erauskin-Extramiana, M., Arrizabalaga, H., Hobday, A. J., Cabré, A., Ibaibarriaga, L., Arregui, I., Murua, H., & Chust, G. (2019). Large-scale distribution of tuna species in a warming ocean. *Global Change Biology*, *25*(6), 2043–2060. https://doi.org/10.1111/gcb.14630

Falco, C. De, Desbiolles, F., Bracco, A., & Pasquero, C. (2022). *Island Mass Effect : A Review of Oceanic Physical Processes*. *9*(July), 1–21. https://doi.org/10.3389/fmars.2022.894860

Faye, S., Lazar, A., Sow, B. A., & Gaye, A. T. (2015). A model study of the seasonality of sea surface temperature and circulation in the Atlantic North-eastern Tropical Upwelling System. *Frontiers in Physics*, *3*(SEP), 1–20. https://doi.org/10.3389/fphy.2015.00076

Fernandes, M. J., Lázaro, C., Santos, A. M. P., & Oliveira, P. (2005). Oceanographic characterisation of the cape verde region using multisensor data. *European Space Agency, (Special Publication) ESA SP*, *572*, 815–824.

Fernández-González, C., Tarran, G. A., Schuback, N., Woodward, E. M. S., Arístegui, J., & Marañón, E. (2022). Phytoplankton responses to changing temperature and nutrient availability are consistent across the tropical and subtropical Atlantic. *Communications Biology*, *5*(1), 1–14. https://doi.org/10.1038/s42003-022-03971-z

Friedland, K. D., Stock, C., Drinkwater, K. F., Link, J. S., Leaf, R. T., Shank, B. V., Rose, J. M., Pilskaln, C. H., & Fogarty, M. J. (2012). Pathways between primary production and fisheries yields of large marine ecosystems. *PLoS ONE*, *7*(1). https://doi.org/10.1371/journal.pone.0028945

Gama, C., Tchepel, O., Baldasano, J. M., Basart, S., Ferreira, J., Pio, C., Cardoso, J., & Borrego, C. (2015). Seasonal patterns of Saharan dust over Cape Verde - a combined approach using observations and modelling. *Tellus, Series B: Chemical and Physical Meteorology*, *67*(1), 1–21. https://doi.org/10.3402/tellusb.v67.24410

Gove, J. M., McManus, M. A., Neuheimer, A. B., Polovina, J. J., Drazen, J. C., Smith, C. R., Merrifield, M. A., Friedlander, A. M., Ehses, J. S., Young, C. W., Dillon, A. K., & Williams, G. J. (2016). Near-island biological hotspots in barren ocean basins. *Nature*

Communications, *7*, 1–8. https://doi.org/10.1038/ncomms10581

Hamne, W. M., & Hauri, I. R. (1981). Effects of island mass: Water flow and plankton pattern around a reef in the great barrier reef lagoon, Australia. *Limnology and Oceanography*, *26*(6), 1084–1102. https://doi.org/10.4319/lo.1981.26.6.1084

Hu, C., Lee, Z., & Franz, B. (2012). Chlorophyll a algorithms for oligotrophic oceans: A novel approach based on three-band reflectance difference. *Journal of Geophysical Research: Oceans*, *117*(1), 1–25. https://doi.org/10.1029/2011JC007395

Jena, B. (2016). Satellite remote sensing of the island mass effect on the Sub-Antarctic Kerguelen Plateau, Southern Ocean. *Frontiers of Earth Science*, *10*(3), 479–486. https://doi.org/10.1007/s11707-016-0561-8

Krasnopolsky, V., Nadiga, S., Mehra, A., Bayler, E., & Behringer, D. (2016). Neural networks technique for filling gaps in satellite measurements: Application to ocean color observations. *Computational Intelligence and Neuroscience*, *2016*. https://doi.org/10.1155/2016/6156513

Lathuilière, C., Echevin, V., & Lévy, M. (2008). Seasonal and intraseasonal surface chlorophyll-a variability along the northwest African coast. *Journal of Geophysical Research: Oceans*, *113*(5), 2000–2004. https://doi.org/10.1029/2007JC004433

Lázaro, C., Fernandes, M. J., Santos, A. M. P., & Oliveira, P. (2005). Seasonal and interannual variability of surface circulation in the Cape Verde region from 8 years of merged T/P and ERS-2 altimeter data. *Remote Sensing of Environment*, *98*(1), 45–62. https://doi.org/10.1016/j.rse.2005.06.005

Li, G., Chen, X., Lei, L., & Guan, W. (2014). Distribution of hotspots of chub mackerel based on remote-sensing data in coastal waters of China. *International Journal of Remote Sensing*, *35*(11–12), 4399–4421. https://doi.org/10.1080/01431161.2014.916057

Li, W., El-Askary, H., ManiKandan, K. P., Qurban, M. A., Garay, M. J., & Kalashnikova, O. V. (2017). Synergistic use of remote sensing and modeling to assess an anomalously high chlorophyll-a event during summer 2015 in the South Central Red Sea. *Remote Sensing*, *9*(8). https://doi.org/10.3390/rs9080778

Martin, S. (2014). Ocean color. In *An Introduction to Ocean Remote Sensing*. https://doi.org/10.1017/cbo9781139094368.009

Martinez, E., & Maamaatuaiahutapu, K. (2004). Island mass effect in the Marquesas Islands:

Time variation. *Geophysical Research Letters*, *31*(18), 1–4. https://doi.org/10.1029/2004GL020682

Martinez, E., Raapoto, H., Maes, C., & Maamaatuaihutapu, K. (2018). Influence of tropical instability waves on phytoplankton biomass near the Marquesas islands. *Remote Sensing*, *10*(4), 1–12. https://doi.org/10.3390/rs10040640

Masunaga, R., & Schneider, N. (2022). Surface Wind Responses to Mesoscale Sea Surface Temperature over Western Boundary Current Regions Assessed by Spectral Transfer Functions. *Journal of the Atmospheric Sciences*, *79*(6), 1549–1573. https://doi.org/10.1175/JAS-D-21-0125.1

Messié, M., Petrenko, A., Doglioli, A. M., Martinez, E., & Alvain, S. (2022). Basin-scale biogeochemical and ecological impacts of islands in the tropical Pacific Ocean. In *Nature Geoscience* (Vol. 15, Issue 6). https://doi.org/10.1038/s41561-022-00957-8

Minas, H. J., Minas, M., & Packard, T. T. (1986). Productivity in upwelling areas deduced from hydrographic and chemical fields. *Limnology and Oceanography*, *31*(6), 1182–1206. https://doi.org/10.4319/lo.1986.31.6.1182

Muskananfola, M. R., Jumsar, & Wirasatriya, A. (2021). Spatio-temporal distribution of chlorophyll-a concentration, sea surface temperature and wind speed using aqua-modis satellite imagery over the Savu Sea, Indonesia. In *Remote Sensing Applications: Society and Environment* (Vol. 22). https://doi.org/10.1016/j.rsase.2021.100483

Pradhan, Y., Lavender, S. J., Hardman-Mountford, N. J., & Aiken, J. (2006). Seasonal and inter-annual variability of chlorophyll-a concentration in the Mauritanian upwelling: Observation of an anomalous event during 1998-1999. *Deep-Sea Research Part II: Topical Studies in Oceanography*, *53*(14–16), 1548–1559. https://doi.org/10.1016/j.dsr2.2006.05.016

Ramalho, R. A. S. (2011). *Building the Cape Verde Islands*. Springer Berlin Heidelberg. https://doi.org/10.1007/978-3-642-19103-9

Ramos, V., -Marrero, J. P., Llinás, O., Cianca, A., & Morales, J. (2012). *Variation of the chlorophyll a related to sea surface temperature, wind and geostrophic currents in the Cape Verde region using satellite data*.

Shafeeque, M., Shah, P., Platt, T., Sathyendranath, S., Menon, N. N., Balchand, A. N., & George, G. (2019). Effect of Precipitation on Chlorophyll-a in an Upwelling Dominated

Region Along the West Coast of India. *Journal of Coastal Research*, *86*(sp1), 218–224. https://doi.org/10.2112/SI86-032.1

Shiozaki, T., Kodama, T., & Furuya, K. (2014). Large-scale impact of the island mass effect through nitrogen fixation in the western South Pacific Ocean. *Geophysical Research Letters*, *41*(8), 2907–2913. https://doi.org/10.1002/2014GL059835

Siswanto, E., Horii, T., Iskandar, I., Gaol, J. L., Setiawan, R. Y., & Susanto, R. D. (2020). Impacts of climate changes on the phytoplankton biomass of the Indonesian Maritime Continent. *Journal of Marine Systems*, *212*(March), 103451. https://doi.org/10.1016/j.jmarsys.2020.103451

Spring, S. (2019). *NOAA Atlas NESDIS 83 WORLD OCEAN ATLAS 2018 Volume 3 : Dissolved Oxygen , Apparent Oxygen Utilization , and Dissolved Oxygen Saturation NOAA National Centers for Environmental Information*. *3*(July).

Vantrepotte, V., & Mélin, F. (2009). Temporal variability of 10-year global SeaWiFS time-series of phytoplankton chlorophyll a concentration. *ICES Journal of Marine Science*, *66*(7), 1547–1556. https://doi.org/10.1093/icesjms/fsp107

Wang, J., Zhang, Y., Yang, F., Cao, X., Bai, Z., Zhu, J., Chen, E., Li, Y., & Ran, Y. (2015). Spatial and temporal variations of chlorophyll-a concentration from 2009 to 2012 in Poyang Lake, China. *Environmental Earth Sciences*, *73*(8), 4063–4075. https://doi.org/10.1007/s12665-014-3691-x

1. https://hermes.acri.fr/index.php?class=archive
2. https://oceancolor.gsfc.nasa.gov